GALLIUM ARSENIDE and RELATED COMPOUNDS 1991

Institute of Physics Conference Series Number 120

Gallium Arsenide and Related Compounds 1991

Conference Committee
Chairman: L R Dawson (Sandia National Labs)
Program Chairman: G B Stringfellow (University of Utah)
Past Chairman: G E Stillman (University of Illinois)
Secretary: H Goronkin (Motorola)
Treasurer: J S Harris (Stanford University)
Awards Chairman: J Woodall (IBM)
Local Arrangements: A G Thompson (Boeing HT Ctr.)

Organizing Committee
R D Burnham (Amoco)
A Y Cho (AT&T Bell Labs)
L R Dawson (Sandia National Labs)
H Goronkin (Motorola)
J S Harris (Stanford University)
V G Keramidas (Bellcore)
P E Norris (EMCORE)
Y S Park (Office of Naval Research)
M Reed (Yale University)
G B Stringfellow (University of Utah)
C M Wolfe (Washington University)
J Woodall (IBM)

Technical Program Committee
G B Stringfellow, Chairman (University of Utah)
N Bottka (Naval Research Labs)
L R Dawson (Sandia National Labs)
C G Fonstad (MIT)
H Goronkin (Motorola)
A C Gossard (UCSB)
J S Harris (Stanford University)
T Ikoma (University of Tokyo)
B A Joyce (Imperial College)
V G Keramidas (Bellcore)
T F Kuech (University of Wisconsin)
Y S Park (Office of Naval Research)
G E Stillman (University of Illinois)
W Tsang (AT&T Bell Labs)
G L Witt (AFOSR)
D J Wolford (IBM)

International Advisory Committee
Chairman: Don W Shaw (Texas Instruments)
Vice Chairman: Takuo Sugano (University of Tokyo)
A Christou (Naval Research Laboratory)
L R Dawson (Sandia National Labs)
Lester Eastman (Cornell University)
Toshiaki Ikoma (University of Tokyo)
John Magarshak (Thompson-TCM—France)
Tsuneo Nakahara (Sumitomo Electric Industries)
Hans S Rupprecht (Fraunhofer Institute—Germany)
Gregory E Stillman (University of Illinois)
Michiyuki Uenohara (Nippon Electric Co., Ltd.)
Bryan Wilson (Plessey Research—UK)

Gallium Arsenide and Related Compounds 1991

Proceedings of the Eighteenth International Symposium on Gallium Arsenide and Related Compounds, Seattle, Washington, USA, 9–12 September 1991

Edited by G B Stringfellow

Institute of Physics Conference Series Number 120
Institute of Physics, Bristol, Philadelphia and New York

0305-2346/92 $4.50+.00

CODEN IPHSAC 120 1–650 (1992)

British Library Cataloguing in Publication Data are available

ISBN 0-85498-410-0

Library of Congress Cataloging-in-Publication Data are available

Published under The Institute of Physics imprint by IOP Publishing Ltd
Techno House, Redcliffe Way, Bristol BS1 6NX, England
335 East 45th Street, New York, NY 10017-3483, USA
US Editorial Office: IOP Publishing Inc., The Public Ledger Building,
Suite 1035, Independence Square, Philadelphia, PA 19106, USA

Printed in Great Britain by Galliard (Printers) Ltd, Great Yarmouth, Norfolk

GaAs Symposium Award and Heinrich Welker Gold Medal

The Gallium Arsenide Symposium Award was initiated in 1976. Candidates for the Award are selected by the GaAs Symposium Award Committee from those who have distinguished themselves in the area of III–V compound semiconductors. The Award consists of $2500 and a plaque citing the recipient's contribution to the field. In addition, the Heinrich Welker Gold Medal, sponsored by Siemens, is also presented to the Award recipient.

The 1976 Award was presented to Nick Holonyak of the University of Illinois for his work leading to the development of the first practical light-emitting diodes and his continuing research on III–V compound semiconductors. The second Award was received by Cyril Hilsum of the Royal Signals and Radar Establishments (now at GEC Research Laboratories) for his contributions in the field of transferred-electron logic devices and the advancement of GaAs MESFETS. In 1981 the Award and Medal were presented to Gerald L Pearson, Stanford University, for his research and teaching in the field of compound semiconductor physics and new device technology. In 1982, the Award and Medal were presented to Herbert Kroemer, University of California at Santa Barbara, for his contributions to hot-electron effects, the Gunn Oscillator, and III–V heterojunction devices including the heterojunction laser. The 1984 Award and Medal were presented to Izuo Hayashi (now at Optoelectronics Joint Research Laboratories) for his contributions to the development and understanding of room temperature operation double-heterojunction lasers. In 1985, the recipient was Heinz Beneking, Technical University of Aachen, in recognition of his distinguished contributions to the development of III–V compound semiconductor technology and new structure devices. In 1986, the Award and Medal were presented to Alfred Y Cho, AT&T Bell Laboratories, for his pioneering work in the development of molecular beam epitaxy and contributions to III–V compound semiconductor research. Zhores I Alferov of the A F Ioffe Technical Institute was the recipient of the Award and Medal in 1987 for his outstanding contributions in liquid phase epitaxy, laser diodes, vapor phase epitaxy, and for innovative contributions to the technology of compound semiconductors. The 1988 GaAs Symposium Award and Welker Medal were presented to Jerry Woodall for his pioneering work in introducing the III–V alloy, AlGaAs, and his further fundamental contributions to III–V compound semiconductor physics. In 1989 the Award and Medal were presented to Don Shaw of Texas Instruments in recognition of his pioneering work in elucidating the complex mechanisms of epitaxial crystal growth using chemical vapor deposition. In 1990 the recipient was Gregory S Stillman of the University of Illinois for his outstanding contributions to the characterization of high-purity GaAs and related compounds and to the understanding and development of near infrared avalanche photodetectors.

At this meeting the 1991 GaAs Symposium Award and Welker Medal were presented to Lester F Eastman in recognition of his many contributions to III–V compound semiconductors, including the development of the concept of ballistic

electron transport, the planar doping technique, the buffer layer technique, and AlInAs/GaInAs/InP heterostructures.

Dr Eastman was born in Utica, NY, and obtained B.S. (1953), M.S. (1955), and Ph.D. (1957) degrees at Cornell University. He joined the faculty of Electrical Engineering at Cornell in 1957. Since 1965 he has been doing research on compound semiconductor materials, high-speed devices, and circuits, and has been active in organizing workshops and conferences on these subjects at Cornell from 1977. In 1977 he joined other Cornell faculty members in obtaining funding and founding the National Research and Resource Facility at Cornell (now the National Nanofabrication Facility). Also in 1977 he founded the Joint Services Electronics Program and directed it until 1987. He has recently joined with others at Cornell to develop a large effort in high-frequency/high-speed optoelectronics. During the 1978–1979 year he was on leave at MIT's Lincoln Laboratory, and during the 1985–1986 year he was at the IBM Watson Research Laboratory. During 1983 he was the IEEE Electron Device Society National Lecturer. He was a member of the U.S. Government Advisory Group on Electron Devices from 1978–1988, and serves as a consultant for several industrial laboratories. He was a founder in 1985 and is now chairman of the board of directors of Northeast Semiconductors, Inc. He has been a Fellow of IEEE since 1969, a member of the National Academy of Engineering since 1986, and was appointed the John L Given Foundation Professor of Engineering at Cornell in January, 1985.

Young Scientist Award

In 1986 the International Advisory Committee of the GaAs and Related Compounds Symposium established a Young Scientist Award to recognize technical achievements in the field of III–V compound semiconductors by a scientist under the age of 40. The Award consists of $1000 and a plaque citing the recipient's contributions. The first Young Scientist Award was presented at the 1986 Symposium to Russell D Dupuis for his work in the development of organometallic vapor phase epitaxy for III–V compound semiconductors.

In 1987 the Award was presented to Dr Naoki Yokoyama for his contributions to developing self-aligned gate technology for GaAs MESFETs and ICs and the resonant tunneling hot-electron transistor. At the 1988 conference, the Young Scientist Award was presented to Won Tsang for his distinguished contributions to the development of new MBE growth techniques and heterostructure devices. The 1989 Award was presented to Russel Fischer in recognition of his work in showing state of the art performance at DC and microwave frequencies of MESFETs, MODFETs, and HBTs using GaAs on Si. In 1990 the Award was made to Yasuhiko Arakawa for his pioneering studies of low-dimensional semiconductor lasers, particularly in regard to his prediction and demonstration of the superiority of quantum wire and quantum box configurations.

At this conference the 1991 Young Scientist Award was presented to Sandip Tiwari of the IBM Watson Research Center in recognition of contributions to the understanding and development of compound semiconductor devices, most notably the metal–semiconductor field effect transistor, the heterostructure field effect transistor, and the heterostructure bipolar transistor.

Dr Tiwari was born in 1955. He attended the Indian Institute of Technology at Kanpur, India, Rensselaer Polytechnic Institute, and Cornell University, where he received his Ph.D. degree in electrical engineering in 1980. He is a Research Staff Member at IBM Watson Research Center working in the area of Semiconductor Physics and Devices.

Dr Tiwari's contributions to the understanding and development of electronic and optical compound semiconductor devices is recorded in over 50 publications and 10 patents. These contributions have included, individually and in collaboration, new device ideas such as p-channel HFETs, SiGe HBTs, and unpinned oxide-based MOSFETs; new technologies such as p-type and n-type refractory ohmic contacts that are readily amenable to self-alignment; and an understanding of new phenomena in devices such as the alloy-potential-related high-current effect in graded heterostructure collector HBTs.

During 1988–1989 he was a Visiting Associate Professor at the University of Michigan. He has been Associate and Guest Editor of the IEEE Transactions on Electron Devices and is the author of the textbook *Compound Semiconductor Device Physics* published by Academic Press.

Preface

This volume presents the papers from the 18th International Symposium on Gallium Arsenide and Related Compounds, held in Seattle, Washington from September 9 to 12, 1991. It includes current results on the materials, characterization, and device aspects of a broad range of semiconductor materials, particularly the III–V compounds and alloys.

The conference consisted of 3 plenary talks, 117 oral presentations, 24 poster papers, and 6 late news papers. The competition was stiff, with less than 50% of the submitted abstracts accepted for presentation at the conference. Consequently, the results included in this volume are timely and of the very highest quality.

The volume is organized with the plenary papers presented in the first chapter, the late news papers in the last chapter (in order to allow the most rapid publication schedule), and the other papers presented by topic in the remaining chapters. Naturally, some papers could be classified in several categories. Thus, the reader is encouraged to peruse the entire volume.

Finally, the editor wishes to especially thank the program committee, listed in the front of the volume, for their hard work in selecting the plenary speakers, deciding which abstracts should be accepted, and having the papers reviewed. Thanks also go to Kathryn Cantley for her invaluable assistance at the conference.

G B Stringfellow

Acknowledgments

The organizers of the Symposium gratefully acknowledge financial support provided by:

AFOSR
AIXTRON
BANDGAP TECHNOLOGY CORP
BOEING SCIENCE AND TECHNOLOGY CENTER
EPI
FISONS INSTRUMENTS
INTEVAC
IEEE
SIEMENS

Contents

Chapter 4: Processing

Chapter 6: HBTs and InGaAlAs FETS

Chapter 8: Ordering

Chapter 9: Quantum Wells

Chapter 10: Opto-electronics

Inst. Phys. Conf. Ser. No 120: Chapter 1
Paper presented at Int. Symp. GaAs and Related Compounds, Seattle, 1991

New directions for III–V structures: metal/semiconductor heteroepitaxy

J P Harbison, T Sands, C J Palmstrom, T L Cheeks, L T Florez, and V G Keramidas

Bellcore, 331 Newman Springs Road, Red Bank, N.J. 07701-7040

ABSTRACT: Epitaxial metallic films grown on semiconductor substrates are most attractive when they consist of materials which are thermodynamically stable with respect to the underlying semiconductor. This allows, under the proper growth conditions, the overgrowth of epitaxial semiconductor layers, thus forming monocrystalline semiconductor/metal/semiconductor heterostructures with exciting physics and device possibilities. This paper discusses our recent work in the growth of stable and epitaxial metallic layers which meet these stringent criteria on III-V semiconductors. Work on layers sharing either a common group III element with the III-V, such as AlAs/NiAl/AlAs or a common group V, such as GaAs/ErAs/GaAs, will be presented. The potential applications are further enhanced when the metallic films display an added functionality such as ferromagnetic behavior, demonstrated in epitaxial MnAl/AlAs/GaAs heterostructures. Examples of new directions for III-V structures made possible by such heteroepitaxy, are discussed. They include tailoring of Schottky barrier heights, integration of metallic quantum wells into high-speed three-terminal devices, and integration of magnetic storage functionality with III-V electronics.

1. INTRODUCTION

The increasingly versatile ability to successfully grow epitaxially material heterostructures which are dissimilar in terms of crystal structure, chemical bonding and even overall physical properties, has led to a wide range of possibilities in the use of this ever widening range of materials combinations. In the two decades since the First International Symposium on GaAs and Related Compounds, the concept of "related compounds" has expanded considerably. That original group, which included only a small list of closely-related lattice-matched III-V compounds, now can truthfully be said to include a broad spectrum of materials ranging from other III-V, II-VI and group IV semiconductors, to epitaxially-grown insulators, high T_c superconductors and metals. It is this last metals category that this paper addresses. We explore some of our current capabilities in forming integral metal/semiconductor monocrystalline structures, and show a few examples of how these new combinations point to new directions for III-V heteroepitaxy.

2. MOTIVATION

The motivation for exploring the concept of buried epitaxial metal layers in III-V heterostructures is multifaceted. The first reason is as an extension of the principle role metallizations already play in III-V devices, that is providing the link between the semiconductor devices and the "outside world" . Until recently, in most cases thermally unstable and polycrystalline metallizations have been adequate for most Schottky barrier and ohmic contact applications. However, we are fast reaching the limits of such schemes. As both lateral and vertical device dimensions "shrink" to the size of the individual metallic grains, the necessity for more controllable single crystal metal substitutes becomes more and more apparent. In addition, the ability to bury metal interconnect layers and ground planes provides a vehicle for increasing the flexibility of device design, leading a step closer to the long sought goal of true three-dimensional device integration. Such combinations would make possible the use of metallic films to provide not only conventional but also more demanding metal/semiconductor functions.

The second motivation is to explore the incorporation of metals into novel, non-traditional device concepts, enhancing the versatility of III-V devices. This class of applications would include metal elements which could be used as magnetic storage devices, buried heat sinks, reflectors or waveguides. As the size of a buried metal layer becomes comparable to the size of the electron wavefunction in the metal, quantum effects begin to dominate, opening up the possibility of metallic quantum wells. Incorporating these in a three terminal

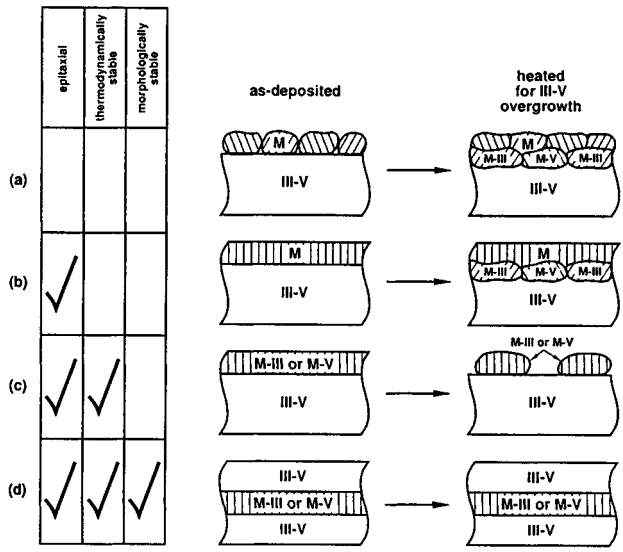

Figure 1: A schematic representation of the three criteria which must be met to allow the formation of a stable, and epitaxial buried metal layer within a III-V heterostructure.

resonant tunneling transistor with a metallic quantum well base, or using metal layers as buried gates in devices, such as an epitaxial permeable base transistor, increases the range of utilization of III-V-based devices. The challenge to the crystal grower is to conquer the complex materials issues so as to achieve the level of perfection in both the buried metal layer itself and the III-V material grown above it for the structures to meet the demanding performance requirements of these novel classes of devices.

3. STABILITY REQUIREMENTS

The rather stringent stability requirements which must be met in choosing a metal which can withstand the elevated temperatures needed to regrow III-V material above it have been thoroughly discussed by Sands et al (1990a). As shown schematically in Figure 1, the metal first of all must have the appropriate structure so as to grow epitaxially on the III-V. This is essential for subsequent monocrystalline III-V overgrowth, necessary for most device applications. Such a requirement alone, however, is still insufficient because, unless the metal is thermodynamically stable with respect to the surrounding III-V, it will eventually react with the underlying III-V when heated for overgrowth, as shown schematically on the right of case b) in the figure. Eventually it will be consumed by the reaction products and thus lose its role as an epitaxial template for the III-V overgrowth above it. If a metal meets these first two criteria, as shown in case c), it may still be unsuitable if it tends to agglomerate upon heating (as shown in the right-hand panel) because it will lose its electrical continuity, essential for most buried metal applications. Only when it is also morphologically stable to agglomeration, will it be possible to successfully achieve III-V overgrowth, retaining the metal layer intact as a continuous thin film.

The most obvious first candidates are the various elemental metals, especially those used in conventional compound semiconductor metallization applications. Although a number of elements meet at least one of the requirements listed above, only a few, such as W which is both morphologically and thermodynamically stable but not epitaxial, or Ag which is epitaxial and relatively thermodynamically stable but not morphologically stable, meet two of the three requirements. None of the elements, with the sole exception of Si, meet all three. And though GaAs on Si and Si delta-doping of GaAs both are legitimate active fields of study in the area of heteroepitaxy, Si can't be considered a viable candidate as a buried metal layer in GaAs. So we need to turn to metallic compounds in order to simultaneously meet all three buried metal layer requirements.

Again, the choices of the proper metallic compounds has been treated in detail in our previous review (Sands et al 1990a). The essence of the choice is indicated schematically in Figure 1. If one chooses M-III or M-V compounds which are the final by-products of an annealing reaction of the semiconductor with a deposited metal, one is then assured of thermodynamic stability. Selecting only those reaction products which form in a single epitaxial relationship with the underlying GaAs insures that the epitaxial requirement is met. And lastly, choosing a metallic compound with as high a melting point as possible allows the substrate to be heated to correspondingly higher temperatures, needed for III-V overgrowth, before entering a regime with high enough metal surface mobility to allow agglomeration.

The materials we have studied most closely which fall into the above categories, are the rare-earth monoarsenides such as ErAs, which form NaCl-type cubic M-V compounds (Palmstrom et al 1988, 1989) and NiAl and CoAl which form CsCl cubic M-III compounds (Harbison et al 1988, Sands et al 1990b). All three compounds have successfully been grown epitaxially (Sands et al 1990a), and though in all three cases the lattice constant of the metals is 1-2% larger than that of GaAs, exact lattice matching to the III-V can be achieved through ternary alloying of either the metal, in the case of $Sc_{.32}Er_{.68}As$ lattice matched to GaAs (Palmstrom et al 1990a), or the III-V in the case of NiAl or CoAl lattice matched to $In_{.30}Ga_{.70}As$ or $In_{.17}Ga_{.83}As$, respectively (Harbison et al 1990).

4. GROWTH BY MOLECULAR BEAM EPITAXY

The growth of these buried metal structures using molecular beam epitaxy (MBE) has been reviewed previously in detail (Sands et al 1990a). The growth sequence for the buried rare-earth monoarsenide/III-V heterostructures is similar to conventional III-V MBE in that the group V source remains on constantly. The group III and rare-earth sources are opened sequentially to build the appropriate buried metal structure. Buried ErAs layers as thin as two monolayers thick which are electrically continuous can be formed, as shown in Figure 2 (Sands et al 1990a). A problem arises, however, when one attempts GaAs overgrowth. Due to unfavorable interface surface energies, the overgrown GaAs grows in a 3-D growth mode, resulting in islands elongated along the [110] and [1$\bar{1}$0] directions, which grow to be many several nanometers thick before they laterally coalesce and

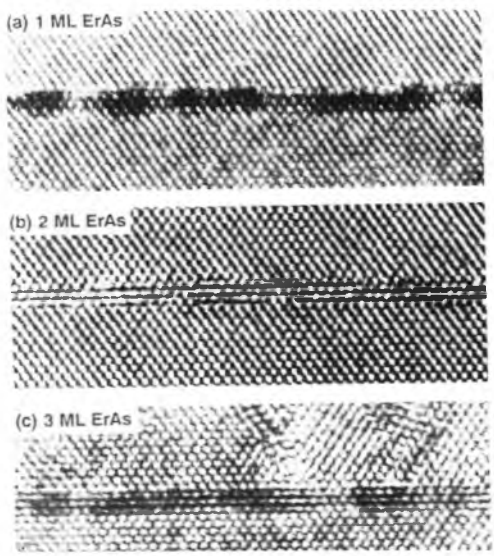

Figure 2: High-resolution cross-sectional transmission electron micrographs comparing buried layers of ErAs in GaAs with average ErAs thicknesses of 1,2 and 3 monolayers. The films are already electrically continuous over macroscopic dimensions by the middle 2 monolayer stage.

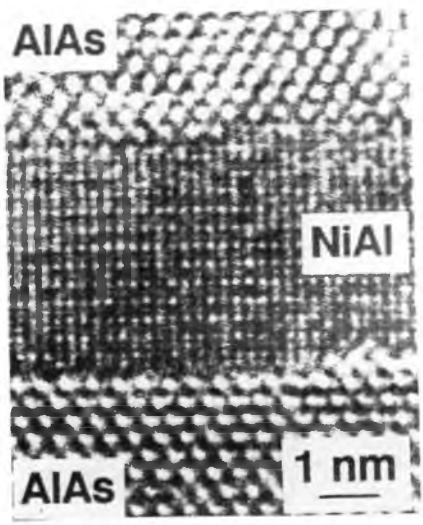

Figure 3: High-resolution cross-sectional transmission electron micrograph showing an epitaxial III-V/NiAl/III-V heterostructure fabricated by MBE (Sands et al 1990a).

completely cover the exposed ErAs. As a result, undesirable twinned GaAs variants form above the ErAs, leading to unwanted defects at the upper metal/semiconductor interface. Though a good fraction of these defects self-annihilate farther on in the overgrowth, their presence at the critical metal/III-V interface, is in general undesirable.

Realizing that this phenomenon was a wetting problem driven primarily by surface and interface energy considerations, and knowing that they were attempting to grow a polar (100) GaAs on a non-polar (100)ErAs surface, Palmstrom et al (1990b) examined the effect of growing on other crystal orientations. While $(\bar{1}\bar{1}\bar{1})$ growth provides polar-on-polar heteroepitaxy, it results in a different problem: the creation of multiple microtwin defects along the $[\bar{1}\bar{1}\bar{1}]$ growth direction in both the rare-earth arsenide and overgrown GaAs layers. By performing growth in the intermediate crystal orientations, $\bar{7}\bar{1}\bar{1}$, $3\bar{1}\bar{1}$, $3\bar{1}\bar{1}$, and $2\bar{1}\bar{1}$, the properties of films with a varying degree of $(\bar{1}\bar{1}\bar{1})$- vs. (100)-like character was explored. While this work is still in progress, preliminary data indicate good growth on these intermediate directions, particularly $(3\bar{1}\bar{1})$, free from the gross defect problems discussed above with respect to straight (100) and $(\bar{1}\bar{1}\bar{1})$ growth.

MBE growth of transition metal aluminides presents difficulties in controlling background arsenic pressure which must be minimized during the intermetallic deposition step (Sands et al 1990a), although there is not as much of a problem in terms of the growth mode of the overgrown III-V. More importantly, special care must be taken to protect the exposed NiAl or CoAl surface from transition metal-arsenide formation during the time needed to raise the As flux again for III-V overgrowth. This may take several minutes. It can, however, be controlled by strategic additions of monolayers of Al during this period which just saturates the impinging As flux and slowly forms a protective AlAs layer. More recently, the advent of valved arsenic cracker MBE sources*, vastly improves the control and response time of the As beam, alleviating many of these problems.

A second issue involves the exclusive nucleation of the (100) NiAl and CoAl variant on the (100) GaAs. Some growth conditions and shutter sequences have been found to nucleate (100) and (110) NiAl variants. By using a template process, however, of initially depositing one monolayer of Ni before codepositing Ni and Al, we can grow now the single desired (100) variant. The same holds true for Co for properly nucleating (100) CoAl. The resulting heterostructure formed when the proper steps are taken to insure the desired orientation of the metal on the III-V and then the III-V on the metal, is shown in Figure 3. Buried metallic films such as these can be made as thin as 1 nm (Sands et al 1990a) and still remain electrically continuous, making them excellent candidates for the metal quantum well devices discussed below.

5. SCHOTTKY BARRIER HEIGHT CONTROL

Having discussed the method we use to fabricate these metal/III-V heterostructures, we will now turn to some of the new directions for III-Vs made possible by such structures. The first direction lies in a more complete control of Schottky barrier height, one of the key parameters in III-V device design. Though many devices could benefit from a controllably high Schottky barrier height, Φ_B, the range of Φ_B values achievable in metallizations deposited by conventional III-V processing remains quite narrow, typically between 0.7 and 0.9 eV. Such metallizations often are not thermodynamically stable in the sense discussed earlier in this article, and they are almost never epitaxial. We have been able to exploit some of the unique properties of these new stable epitaxial metallization systems and provide a greater range of Φ_B. These modified Schottky barriers have thermally stable properties even up into the upper end of III-V processing temperatures (400 - 600 °C).

One way we have been able to tailor the effective Φ_B in the transition metal aluminide system is by controlling the thickness of an AlAs layer inserted between the GaAs and the NiAl or CoAl for chemical stability. Since AlAs has a substantially higher Φ_B for most metallizations ($\Phi_B \sim 1.1$ eV), the Φ_B of the composite metal/AlAs/GaAs heterostructure can be significantly elevated over that of metallizations directly on GaAs. This scheme is similar to using metals deposited ex situ on MBE-grown III-V structures terminated with AlGaAs layers. The advantage in the present case is that pure AlAs can be utilized despite its reactivity in air because the epitaxial metallization is deposited in situ, protecting it from air exposure. Cheeks et al (1991) have shown that the I-V barrier heights in such NiAl/AlAs/GaAs and CoAl/AlAs/GaAs heterostructures can be as high as the 1.1 eV. Furthermore, if the AlAs interlayer is made thin enough to allow electrical tunneling, this effective I-V barrier height can be varied continuously from 0.75 to 1.1 eV, yielding a controllably tailorable Φ_B, by simply varying the thickness of the AlAs tunnel barrier.

Yet another example of increased Φ_B control using the stable epitaxial structures discussed above, which relies fundamentally on the monocrystalline nature of the interface, is the work of Palmstrom et al (1990b, 1992) studying Φ_B as a function of crystal orientation. Tung et al (1989) have shown previously, in the case of monocrystalline silicide/Si heterostructures, that Φ_B can be uniquely determined by the exact atomic

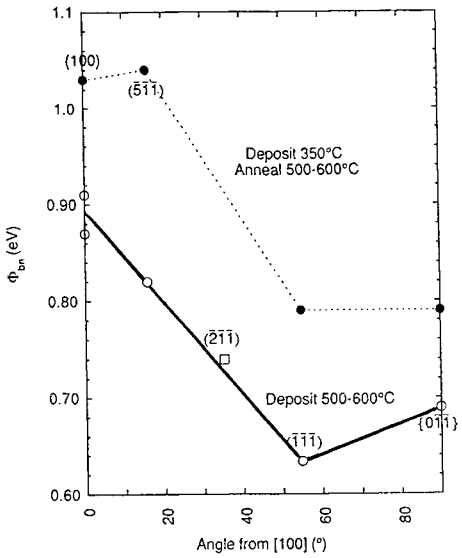

Figure 4: Φ_B for lattice matched ScErAs/GaAs diodes with different GaAs substrate orientation. Thermally stable valves over a range in excess of 0.65 - 1.0 eV are achievable.

arrangement at the single crystal interface. Palmstrom et al (1990b, 1992) rely on such a concept and explore the dependence of Φ_B on the crystallographic orientation of the underlying substrate. The study parallels the overgrowth mode work as a function of orientation discussed above in the previous section. Their results are shown in Figure 4. Because the bonding across the metal/III-V interface is so different for the (100) and ($\bar{1}\bar{1}\bar{1}$) case (nonpolar-on-polar vs. polar-on-polar) it is not surprising that Φ_B is significantly different for these two cases. Figure 4 also shows that one can obtain intermediate values between these two extremes by choosing intermediate crystallographic orientations. Furthermore, additional reproducible differences can be seen between samples deposited at low temperature and annealed at high temperature and ones deposited directly at high temperature (upper and lower curves in the figure). The different As/Ga stoichiometry at the interface determined by the substrate temperature is the probable cause for these differences. The results demonstrate quite a wide swing in Φ_B in excess of 0.65 - 1.0 eV. Furthermore, these Φ_B's are thermally stable up to the 600 °C range, making them applicable to device structures requiring relatively high-temperature processing.

6. METALLIC QUANTUM WELL DEVICES

Another new direction for III-Vs made possible by the fabrication of integral III-V/metal/III-V heterostructures arises from the discrete quantum-confined energy levels which appear in such a metallic quantum well when the metal layer becomes thin enough that it is comparable to the size of the wavefunction of the electron (Sands et al 1990a). The physics which gives rise to the quantum confinement effects is qualitatively quite similar to that in III-V heterostructure quantum wells. The differences are quantitative. Whereas a semiconductor quantum well has a relatively shallow depth of a few tenths of an eV, with intersubband spacings on the order of a tenth of an eV, metallic quantum wells are much deeper, typically 10 eV, with subband spacings on the order of an eV. In addition, the metallic wells have sheet concentrations ~100 times higher than the semiconductor wells (typically $10^{15}/cm^2$ as opposed to $10^{13}/cm^2$) with as many as 10 - 20 of the lowest subbands filled below the Fermi level. This increased carrier density results in a highly desirable decreased sheet resistance which could play a crucial role in devices in which one makes electrical contact to the well itself. Tabatabaie et al (1988) first explored the two terminal vertical transport properties of such metallic quantum wells in the 2-5 nm thickness range, cladding them with two AlAs tunnel barriers surrounded by GaAs. They showed that such a structure behaves like a canonical all-semiconductor double-barrier resonant tunneling diode. One, and on occasion two negative differential resistance regions were detected with peak-to-valley ratios at room temperature as high as 2:1, confirming metallic quantum well behavior.

Tabatabaie et al (1989) took this concept one step further by fabricating a three-terminal switching device based on a contacted metallic quantum well layer, (shown schematically in Figure 5). Processing takes advantage of the fact that the metallic well can be contacted in a straightforward manner using etches selective between the semiconductor and the metal. A low-resistance ohmic Ti-Au contact can easily be made to NiAl through these etch-exposed areas without the need for an annealing step.

The concept of the device is to modulate the current tunneling from the leftmost source through the left hand AlAs barrier into the metallic NiAl quantum well by means of a rightmost gate. Modulating the gate voltage modulates the exact shape of the right hand AlAs barrier, which in turn subtly affects the position of the confined quantum states within the metallic well. Figure 6 shows the operation conditions chosen in such a way that increasing the gate voltage, plotted on the x-axis, pulls a quantum confined state which is in resonance out of resonance, resulting in the measured monotonic decrease in the source current. The flat, near-zero gate current shown in the same figure at an expanded scale on the left, provides proof that the effect does not arise from current injection from the gate side of the device. Though the proportion of the source current modulated in this way due to these quantum effects is quite low in this first proof-of-principle device, the possibilities it suggests for yet other three-terminal metallic quantum well devices are quite rich and varied, providing exciting new directions for the future.

7. INTEGRATED MAGNETIC STORAGE AND III-V ELECTRONICS

The final example of a new direction opened up for III-V's through the use of stable epitaxial metal/semiconductor heterostructures comes in the field of magnetic materials. Many ferromagnetic thin film applications, such as dense perpendicular magnetic recording and magneto-optic recording or switching, require films with a magnetization perpendicular to the film plane. In the current generation of magneto-optic commercial films this is achieved by growth-induced stress anisotropies, not yet completely understood. In ferromagnetic epitaxial films such as Fe and Co, because of the large shape anisotropy of a thin film

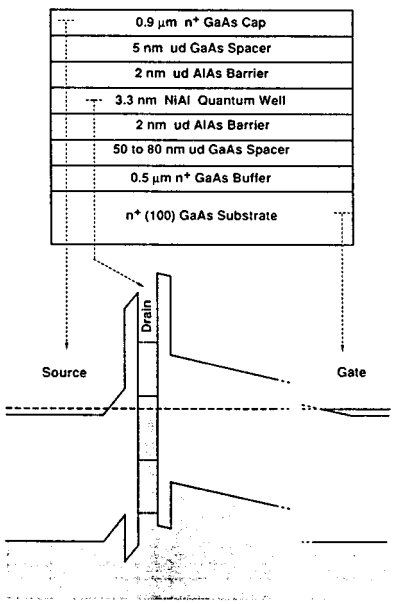

Figure 5: Schematic representation of a successful three-terminal metallic quantum well device dubbed a buried metal well quantum field effect device (Tabatabaie et al 1989).

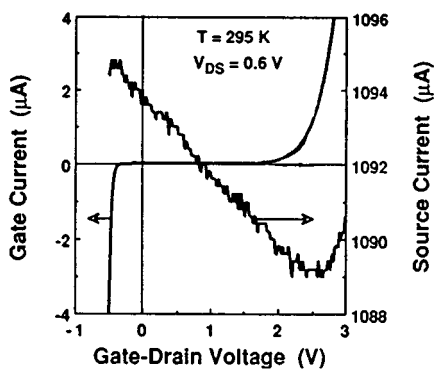

Figure 6: I-V characteristics of the device shown in Figure 5.

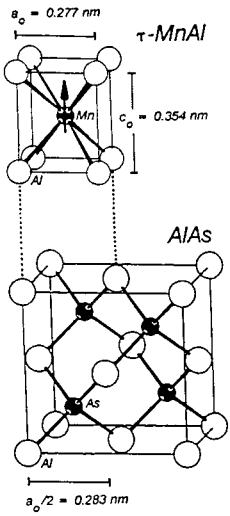

Figure 7: Epitaxial orientation of the ferromagnetic tetragonal τ-MnAl phase on the underlying (100) AlAs layer. Such an orientation leads to perpendicular magnetization desired for many applications (Sands et al 1990c).

geometry, the magnetization inevitably lies in the plane. In the case of τ-MnAl/AlAs/GaAs heterostructures which we have fabricated along the lines of the systems discussed in the above sections of this article, epitaxy has been used to orient the film magnetization perpendicular to the film surface. As shown in Figure 7, the τ-MnAl phase is a tetragonally distorted version of the cubic CsCl structure of NiAl and CoAl. This phase possesses a strong magnetocrystalline anisotropy favoring the alignment of the magnetic moment of the Mn atom along the long axis of the tetragonal cell. By growing the film epitaxially on AlAs with the tetragonal unit cell's square dimensions closely matching the (100) AlAs surface, we can "engineer" this magnetization along the proper plane-perpendicular direction. This τ-phase is the only ferromagnetic phase in the MnAl system. It is, however, a metastable phase accessed previously only by non-equilibrium techniques such as quenching or sputtering. In spite of its inherent metastability, we can use the epitaxial template's alignment energetic advantage to further stabilize this desired magnetic phase. The growth process (Harbison et al 1991), closely parallels that of the other transition metal aluminides and relies heavily, again, on the all important approach of proper initial template formation at the AlAs/MnAl interface.

The magneto-optic properties of these MnAl films are discussed more thoroughly elsewhere in this volume (Cheeks et al 1992). Preliminary measurements of very thin layer films are already within a factor of 2 or 3 of the materials currently in use, with further improvements expected for thicker films. Measurements of the perpendicular magnetic component of the films have also been made using the extraordinary Hall effect, an in-plane transport probe of the film magnetization (Leadbeater et al 1991). Not only do such measurements confirm the existence of a strong perpendicular magnetic component, but in the best films they reveal an almost ideal rectangular magnetic hysteresis loop which is optimal for many magnetic storage applications The films possess a coercive field of a few kilogauss, close to 100% remnance and a Curie temperature in the range of 250 - 400°C. One such trace is shown in the upper right-hand panel of Figure 8. The ability to have magnetic storage on chip in a form integrated with the III-V electronics is very appealing, and represents quite a significant new direction. What makes this particular measurement so appealing, in the context of new directions for III-V's, is that the MnAl being probed was part of an integrated structure, shown in the left-hand side of the figure, which included a two-dimensional electron gas (2DEG) in the underlying III-V. The simultaneous presence of a good 2DEG is evidenced by the Shubnikov de Haas oscillations displayed in the lower right, measured in the underlying semiconductor nearby. The juxtaposition of these two capabilities opens the possibility of future applications in which the non-volatile memory elements in the form of "magnetic gates" may be able to directly affect high-speed switching in underlying circuitry, based perhaps, as in this example, on a 2DEG, forming a switchable channel.

The applications of the new concepts presented here are admittedly some time off in the future. Yet they illustrate some of the powerful new directions being opened up through the newly established capability to grow crystalline metallic thin films and their subsequent use in integrated metal/III-V semiconductor heterostructures.

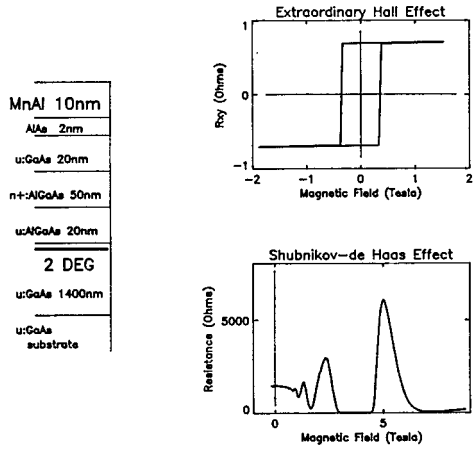

Figure 8: Results of measurements probing both the magnetic hysteresis loop of the MnAl film, using in-plane transverse resistivity referred to as the extraordinary hall effect, and the Shubnikov-de Haas oscillations revealing the presence of a two-dimensional electron gas in the underlying semiconductor portion of the heterostructure. The measurements were made on slightly different sections of the wafer whereby contacts could be made in one area to the magnetic metal film and in the other to the two-dimensional electron gas.

References

* EPI, 261 East Fifth Street, St. Paul, Minnesota, USA 55101

Cheeks T L, Sands T, Nahory R E, Harbison J P, Gilchrist H L and Keramidas V G 1991 accepted for publication in J. Electronic Mat.

Cheeks T L, Nahory R E, Sands T, Harbison J P, Brasil M J S P, Gilchrist H L, Schwartz S, Pudensi M, Allen S J Jr, Florez L T and Keramidas V G 1992 Proceedings of the 18th International Symposium on GaAs and Related Compounds held in Seattle, Washington September 9-12, 1991

Harbison J P, Sands T, Tabatabaie N, Chan W K, Florez L T and Keramidas V G 1988 Appl. Phys. Lett. **53** 1717

Harbison J P, Sands T, Ramesh R, Tabatabaie N, Gilchrist H L, Florez L T and Keramidas V G 1990 J. Vac. Sc. Technol. **B8** 242

Harbison J P, Sands T, Ramesh R, Florez L T, Wilkens B J and Keramidas V G 1991 J. Cryst. Growth **III** 978

Leadbeater M L, Allen S J Jr, DeRosa F, Harbison J P, Sands T, Ramesh R, Florez L T and Keramidas V G 1991 J. Appl. Phys. **69** 4689

Palmstrom C J, Tabatabaie N and Allen S J Jr 1988 Appl. Phys. Lett. **53** 2608

Palmstrom C J, Garrison K C, Mounier S, Sands T, Schwartz C L, Tabatabaie N, Allen S J Jr, Gilchrist H L and Miceli P F 1989 J. Vac. Sci. Techol. **B7** 747

Palmstrom C J, Mounier S, Finstad T G and Miceli P F 1990a Appl. Phys. Lett. **56** 382

Palmstrom C J, Cheeks T L, Gilchrist H L, Zhu J G, Carter C B and Nahory R E 1990b Mat. Res. Soc. Extended Abstract **EA-21** 63

Palmstrom C J, Cheeks T L, Gilchrist H L, Zhu J G and Carter C B 1992 to be submitted to J. Vac. Sci. Technol.

Sands T, Palmstrom C J, Harbison J P, Keramidas V G, Tabatabaie N, Cheeks T L, Ramesh R and Silberberg 1990a Materials Science Reports **5** pp 99-170

Sands T, Harbison J P, Ramesh R, Palmstrom C J, Florez L T and Keramidas V G 1990b Mater. Sci. Eng. **B6** 147

Sands T, Harbison J P, Leadbeater M L, Allen S J Jr, Hull G W, Ramesh R, and Keramidas V G 1990c Appl. Phys. Lett. **57** 2609

Tabatabaie N, Sands T, Harbison J P, Gilchrist H L and Keramidas V G 1988 Appl. Phys. Lett. **53** 2528

Tabatabaie N, Sands T, Harbison J P, Gilchrist H L, Cheeks T L, Florez L T and Keramidas V G 1989 Technical Digest International Electron Device Meeting Dec. 3-6, 1989, Washington DC **IEDM 89** 555

Tung R T 1989 J. Vac. Sci. Technol. **A7** 598

Inst. Phys. Conf. Ser. No 120: Chapter 1
Paper presented at Int. Symp. GaAs and Related Compounds, Seattle, 1991

Short wavelength II–VI laser diodes

M.A. Haase, J. Qiu, J.M. DePuydt and H. Cheng
3M Company, 201-1N-35, 3M Center, St. Paul, MN 55144

Abstract The first wide band gap II-VI semiconductor laser diodes were recently reported. These devices emit at 490 nm (blue-green) under pulsed current injection at 77 K, and are comprised of CdZnSe single quantum wells in ZnSe-ZnSSe waveguides. Further advances in this technology have resulted in room temperature pulsed operation of green laser diodes. These developments are discussed in light of the difficulties which have historically been presented by the II-VI compounds.

Introduction

Research on wide band gap II-VI materials (*i.e.*, ZnSe, which has a band gap of 2.7 eV, and related ternaries) and devices has burgeoned in the last few years. Although there have been interesting reports of attempts to incorporate ZnSe into GaAs electronic devices, the most important applications are as visible light emitters. Blue LEDs may find applications as indicators and in high-brightness full-color displays. Short-wavelength (blue or green) laser diodes are expected to play a major role in next-generation optical recording systems, where the smaller spot size afforded by the short wavelength will allow significantly higher information densities. Such lasers are also likely to be used in laser printers, digital photocopiers, and a wide variety of sensors. Undersea optical communications are often mentioned as another possible application, since the attenuation of blue light in sea water is less than that of any other wavelength in the electromagnetic spectrum.

This paper provides a summary of the salient developments leading to the demonstration of the first wide band gap II-VI laser diodes, operating at wavelengths as short as 490 nm (Haase *et al* 1991b). Three important obstacles stood in the way of this accomplishment. They were—and to a large extent still *are*—1) the difficulty of attaining high *p*-type conductivity in ZnSe and related alloys, 2) the lack of a suitable ohmic contact to *p*-ZnSe, and 3) the need for an appropriate heterostructure system to provide carrier and optical confinement.

1. The quest for p-type ZnSe

Claims of p-type conductivity (albeit, extremely low conductivity) in bulk ZnSe date back at least to 1967 (Haanstra 1967). Perhaps the first truly encouraging report of *p*-type conductivity in ZnSe was the bulk growth of Nishizawa *et al* (1986). They reported hole concentrations up to 1.5×10^{15} cm^{-3} using Li acceptors. The first reports of epitaxial *p*-type ZnSe grown on GaAs came in early 1988. Yasuda *et al* (1988) used MOCVD and Li_3N (presumably the acceptor was Li), and Cheng *et al* (1988) used MBE and elemental Li. One of the more intriguing results was that of Akimoto *et al* (1989), who reported *p*-type doping and *pn* junctions using O acceptors from a ZnO source in MBE. Nitrogen acceptors and *p*-type conductivity were also reported using NH_3 in MOCVD (Ohki *et al* 1988), and MOMBE (Migita *et al* 1990).

Through 1990, the success of ZnSe:Li by MBE was arguably the most reproducible, as it spread to several laboratories and led to several reports of blue LEDs. Despite the widely discussed "problems" of rapid diffusion, and electromigration (Haase et al 1991a), Li doping played an important role by allowing the clear identification of the important issue of (the lack of) ohmic contacts to *p*-ZnSe. For lightly doped *p*-ZnSe, this difficulty makes Hall measurements unreliable, if not impossible. The issue of *p*-type contacts will be discussed in the next section. One of the important outcomes was the conclusion that *C-V* measurements of N_A-N_D are as informative and more reliable than Hall measurements—not to mention easier (DePuydt *et al* 1989). A standard mercury probe used at relatively low frequencies (<10 kHz) suffices. The real problem with ZnSe:Li (at least by MBE) was the fact that at high Li concentrations (above 10^{17} cm^{-3}) compensation occurs. Therefore, N_A-N_D in excess of 1×10^{17} cm^{-3} was never achieved (DePuydt *et al* 1989).

An important breakthrough came with the development of an N_2 plasma source for MBE by Park *et al* (1990), and independently by Ohkawa *et al* (1991). This technique employs a small helical-coil rf plasma chamber (manufactured by Oxford Applied Research) which replaces a Knudsen cell in the MBE chamber. The "active" nitrogen species is thought to be either neutral, mono-atomic N "free radicals," or neutral, excited N_2 molecules. Park *et al* used the technique to achieve N_A-N_D=3.4×10^{17} cm^{-3} and blue LEDs.

Subsequent work by Qiu *et al* (1991) demonstrated N_A-N_D up to 1.0×10^{18} cm^{-3} by doping with a nitrogen-plasma source. In that work we showed that the N incorporation could be increased by: 1.) increasing the rf power, 2.) increasing the II/VI flux ratio, or 3.) by

decreasing the substrate temperature. We also showed that compensation occurs at N concentrations in excess of about 10^{18} cm^{-3}, thus limiting N_A-N_D. The most important discovery of that work was that higher N_A-N_D can be achieved at lower substrate temperatures. The room temperature resistivities of our ZnSe:N layers are as low as 0.7 Ω-cm. We have also made convincing variable-temperature van der Pauw-Hall measurements (DePuydt *et al* 1991).

The reproducibility of our ZnSe:N layers is excellent, and similar results have been achieved in ZnSSe alloys; particularly in $ZnS_{0.07}Se_{0.93}$ which is lattice-matched to GaAs at the growth temperature of 300°C.

2. The ohmic contact problem

The difficulty of making device-quality ohmic contacts to *p*-ZnSe was grossly underestimated by many of the early workers in this field. In early 1990, we (the 3M group) reported in some detail on blue LEDs which operated at over 15V at modest current densities. The problem was identified as difficulty in injecting holes into *p*-ZnSe (Haase *et al* 1990).

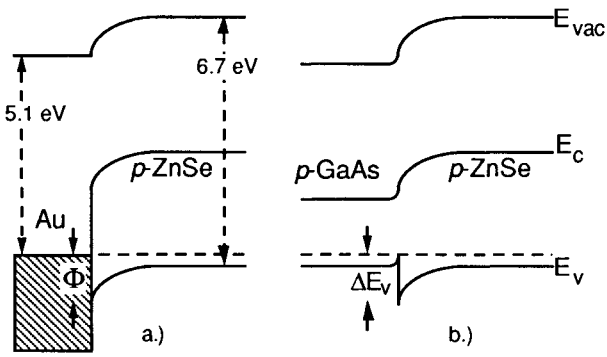

Figure 1. Band diagrams of a.) p-type ZnSe Schottky barrier, and b.) the p-GaAs/p-ZnSe interface.

The fundamental impediment to the injection of holes into *p*-ZnSe is simply that the energy of the valence band is extremely low—approximately -6.7 eV with respect to the vacuum level. Most metals form more-or-less "classical" Schottky barriers on ZnSe and other wide band gap materials. Pt and Au are among the metals with the largest work functions at 5.1 and 5.65 eV, respectively. Therefore, one would expect them to result in Schottky barrier heights Φ of 1.6 and 1.1 eV (Figure 1). In fact, the valence-band barrier height for Au-ZnSe has been measured at 1.25 eV by XPS (Xu *et al* 1988). Our experience

with Pt (sputtered, evaporated, and electroplated) is that it is slightly inferior to Au for hole injection.

We have experimented with many metals (Li, Na, Mg, Ti, Cr, Mn, Ni, Pd, Pt, Cu, Ag, Au, Zn, Hg, Al, In, Sn, Pb, Sb, Bi, and many alloys thereof), surface cleaning techniques (*in situ* evaporation, wet chemical etching, sputter etching), deposition techniques (electroplating, evaporation, sputtering) and annealing techniques (including rapid thermal annealing, and laser annealing). The conclusion is that evaporated, unannealed Au provides the "least bad" contact—that is, the leakiest Schottky barrier.

The III-V materials, *e.g.*, GaAs, provide at least two advantages over ZnSe for making low resistance electrical contacts. First, several metals will alloy with GaAs at reasonable temperatures. Our experience with *p*-ZnSe has shown that the material begins to compensate, becoming more resistive, if heated to temperatures above its growth temperature (typically 300°C). Unfortunately, we have found no metals that alloy at these low temperatures. The other III-V advantage is that degenerate doping is trivial. To make a *p*-type contact, one need only to alloy with a metal that includes Zn to make very heavily *p*-doped material, and achieve large tunneling currents. With the II-VIs, of course, it is much more difficult to make p^+ material.

One might hope that hole injection could be achieved via the III-V to II-VI interface. In this case, the depth of the ZnSe valence bands presents itself as a large band discontinuity, $\Delta E_V \approx 1.0$ eV (Kowalczyk 1982, Kassel 1990), again blocking hole transport (Figure 1). Therefore, if one makes a ZnSe *pn* junction LED (or laser) on a *p*-GaAs substrate, the *p*-GaAs/*p*-ZnSe interface blocks hole flow from the substrate. If sufficient voltage is applied, current flows by avalanche injection at this interface. Filamentary (spotty) injection is observed. In the most heavily doped *p*-ZnSe, the spots are sufficiently dense to give the appearance of uniform emission.

Alternatively, we have made blue LEDs (and blue-green laser diodes) on *n*-GaAs substrates, with the *p*-ZnSe on top. In this case, the reverse-biased Schottky barrier blocks hole injection from the metal electrode. Again, at sufficiently high voltage, current flows by means of avalanche injection. Recently, with the advent of N doping *via* rf plasma, we have used heavily doped (N_A-$N_D \approx 10^{18}$ cm^{-3}) contact layers, and semitransparent Au (100 Å thick) electrodes. The current injection from such structures behaves more like tunneling current, and may be modeled with Fowler-Nordheim theory. The operating voltages of the best LEDs are typically 6 V.

3. Laser design

Recently, the first blue-green laser diodes were announced (Haase *et al* 1991b). In order to achieve sufficient carrier confinement to reach inversion, a single strained quantum well of CdZnSe was used within a ZnSe *pn* junction. CdZnSe-ZnSe quantum wells have been shown to lase by photopumping, although extremely high input powers were required (Ding *et al* 1990).

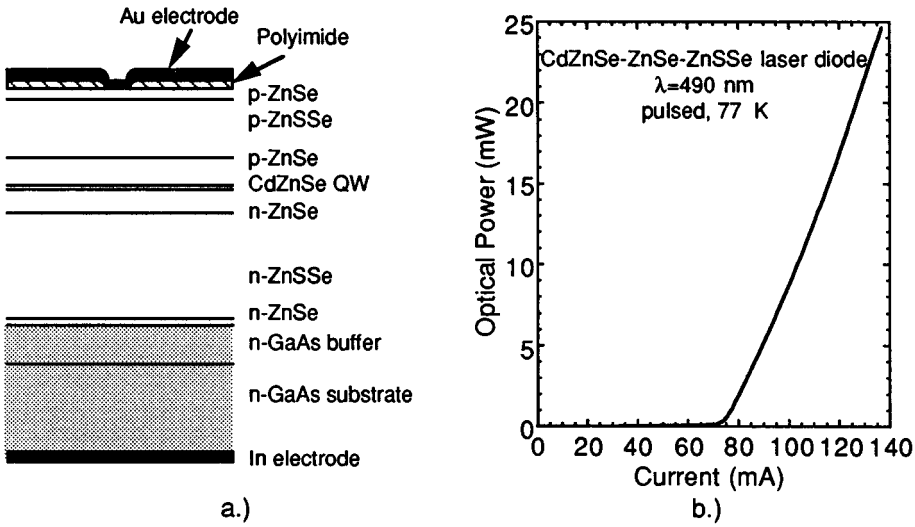

Figure 2. a.) Cross-section of a blue-green laser diode. b.) L-I characteristic of such a device.

The index of refraction of ZnSe is approximately 2.7, which can be compared to 3.9 for GaAs at the operating wavelength of 490 nm (at 77K). Therefore, light generated in the II-VI material tends to be antiguided into the substrate where it is strongly absorbed. Although a lossy waveguide is formed by the discontinuity of the imaginary part of the refractive index, better optical confinement is needed. We have used $ZnS_{0.07}Se_{0.93}$ for a cladding material. A cross section of the device is diagrammed in Figure 2. The top and bottom ZnSSe cladding layers are 1.5 and 2.5 μm thick, respectively, and the total thickness of the ZnSe light-guiding region is 1.0 μm. The $Cd_{0.2}Zn_{0.8}Se$ quantum well is nominally 100 Å thick. The *p*-type layers are doped (from an N_2 plasma source) to N_A-N_D=2×10^{17} cm^{-3}, except for the top 0.1 μm ZnSe layer which is doped to 10^{18} cm^{-3}. The lower *n*-ZnSe guiding layer is doped with Cl from a $ZnCl_2$ source to 1×10^{17} cm^{-3}, and the lower cladding and *n*-ZnSe contact layer to about 10^{18} cm^{-3}. Devices are typically patterned into 20 μm wide "gain-guided" stripes, and cleaved

to cavity lengths typically on the order of 1 mm. The lower index of refraction of ZnSe gives rise to uncoated facet reflectivities of only 0.21 (compared to 0.3 for GaAs lasers).

Computer modeling of the heterostructure shown in Figure 2 shows that the optical confinement is sufficient to reduce losses in the substrate to less than 1 cm^{-1} (much less than the anticipated free carrier and scattering losses), and to provide an optical confinement factor of Γ=0.013 for a 100 Å quantum well.

Because of the persistent *p*-type contact problem, these devices have so far been operated only under pulsed current injection. Laser action was first seen at 77 K, at a wavelength of 490 nm (blue-green). Lasers from that first wafer have worked at temperatures as high as 200 K without facet coatings. Figure 2b shows an *L-I* characteristic for one of these devices. Output powers in excess of 100 mW per facet have been observed. Differential quantum efficiencies in excess of 20% per facet have also been measured. The threshold current for the device of Figure 2b is 78 mA which corresponds to 320 A/cm^2. The output from these devices is TE polarized, and a "speckle pattern" is clearly visible.

Figure 3 shows the characteristic electroluminescence spectra from one of these laser diodes. The devices operate in many longitudinal modes, and several lateral modes.

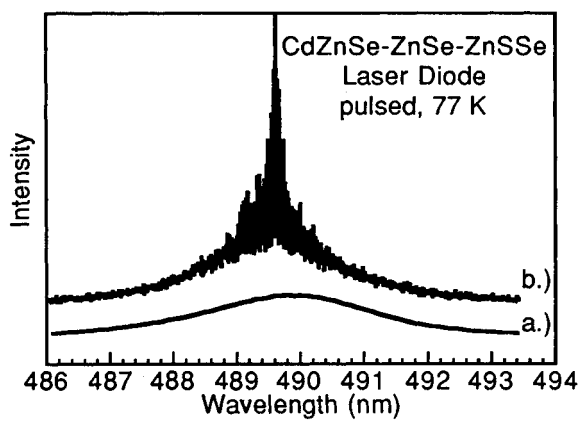

Figure 3. Electroluminescence spectra from a blue-green laser diode: a.) below threshold, b.) above threshold.

In order to achieve operation at room temperature, we have grown a similar structure with a deeper quantum well to enhance the carrier confinement. In this case, the well is nominally 75 Å of $Cd_{0.34}Zn_{0.66}Se$. By coating both facets of the devices made with this material with high reflectivity ($R \approx 0.7$) dielectric coatings (in order to reduce the

gain required for stimulated emission), we have observed 77 K threshold currents as low as 13 mA for a 695 μm long device, which corresponds to 95 A/cm^2. These facet-coated devices also operated at room temperature at a wavelength of 535 nm (green). Figure 4a shows a room temperature *L-I* curve for one of these devices. The threshold current density is about 5000 A/cm^2. Other devices have had threshold current densities as low as 2800 A/cm^2 at room temperature.

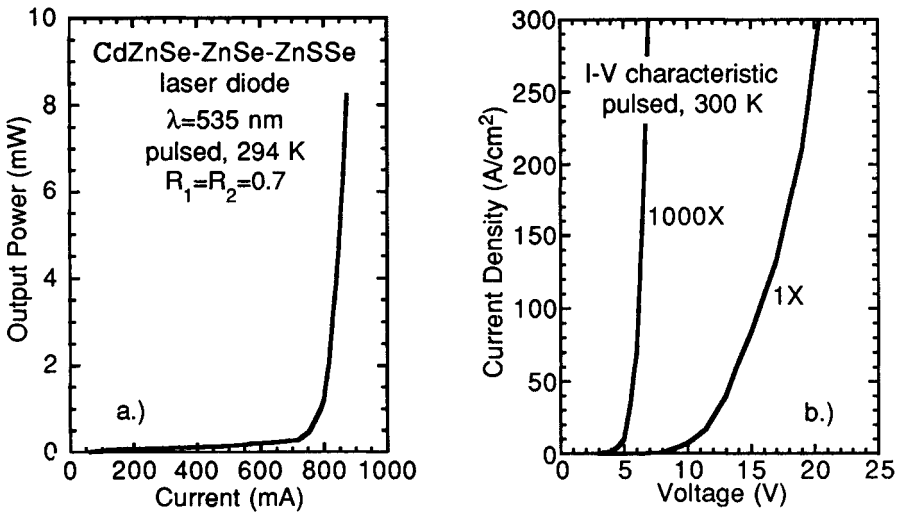

Figure 4. a.) L-I characteristic for a green laser diode at room temperature, b.) I-V characteristic for a II-VI laser diode.

The I-V characteristic for a typical laser diode is shown in Figure 4b. At low current densities, these devices act like well-behaved diodes (with turn-on voltages of 4-5 V). However, to reach the laser threshold current density, 20 V is typically required. This implies that over 10 W of input power is needed to reach threshold at room temperature. It is not surprising that the lifetimes of these lasers are only a few minutes at room temperature.

Conclusions

Recent achievements have clearly demonstrated the feasibility of blue-green laser diodes fabricated from II-VI semiconductors. However, if such devices are to become commercially viable, several outstanding challenges must be met. These include reduction of the room-temperature threshold current densities, and development of low-resistance ohmic contacts to *p*-type ZnSe.

Acknowledgements

We gratefully acknowledge the waveguide modeling of D.K. Misemer, and the technical assistance of K.A. Gleason and P.F. Baude.

References

Akimoto K, Miyajima T and Mori Y 1989b Japan. J. Appl. Phys. **28** L531

Cheng H, DePuydt J M, Potts J E, and Smith T L 1988 Appl. Phys. Lett. **52** 147

DePuydt J M, Haase M A, Cheng H and Potts J E 1989 Appl. Phys, Lett. **55** 1103

DePuydt J M, Haase M A, Qiu J and Cheng H 1991 unpublished.

Ding J, Jeon H, Nurmikko A V, Luo H, Samaranth N and Furdyna J K 1990 Appl. Phys. Lett. **57** 2756

Haanstra J H 1967 in *II-VI Semiconducting Compounds* ed D G Thomas (New York: Benjamin) pp 207-14

Haase M A, Cheng H, DePuydt J M and Potts J E 1990 J. Appl. Phys. **67** 448

Haase M A, DePuydt J M, Cheng H and Potts J E 1991a Appl. Phys. Lett. **58** 1173

Haase M A, Qiu J, DePuydt J M and Cheng H 1991b IEEE Device Research Conference; to be published in Appl. Phys. Lett. **59** (11)

Kassel L, Abad H, Garland J W, Raccah P M, Potts J E, Haase M A and Cheng H 1990 Appl. Phys. Lett. **56** 42

Kowalczyk S P, Kraut E A, Waldrop J R and Grant R W 1982 J. Vac. Sci. Technol. **21** 482

Migita M, Taike A and Yamamoto H 1990 J. Appl. Phys. **68** 880

Ohkawa K, Karasawa T and Mitsuyu T 1991 Japan. J. Appl. Phys. **30** L152

Ohki A, Shibata N and Zembutsu S 1988 Japan. J. Appl. Phys. **27** L909

Park R M, Troffer M B, Rouleau C M, DePuydt J M and Haase M A 1990 Appl. Phys. Lett. **57** 2127

Qiu J, DePuydt J M, Cheng H, and Haase M A 1991 Electronic Materials Conference

Xu F, Vos M, Weaver J H and Cheng H 1988 Phys. Rev. **B38** 13418

Yasuda T, Mitsuishi I and Kukimoto H 1988 Appl Phys. Lett. **52**, 57

Inst. Phys. Conf. Ser. No 120: Chapter 1
Paper presented at Int. Symp. GaAs and Related Compounds, Seattle, 1991

Two-dimensional electron optics in GaAs

H. L. Stormer, J. Spector*, J. S. Weiner, K. W. Baldwin, L. N. Pfeiffer and K. W. West
AT&T Bell Laboratories, Murray Hill, N.J. 07974

Electron mobilities in modulation-doped GaAs-AlGaAs heterostructures presently exceed values of $10^7 cm^2/Vsec$ at low temperatures, equivalent to elastic mean free paths of ~100μm (Pfeiffer *et al* 1989). These are macroscopic distances on the length scale of today's semiconductor fabrication techniques. Electronic transport in such materials can no longer be regarded as diffusive. Instead, low-energy electron propagation is ballistic and a large fraction of the carriers traverse typical device distances without a serious scattering event. On one hand, such extraordinary electronic transport can seriously alter the low-temperature performance of traditional devices that are based on high mobility 2D electron systems. On the other hand, ballistic propagation offers novel possibilities to control and manipulate electrons in such systems.

Research of the past few years shows that low-energy ballistic carriers in two-dimensional electron systems behave in many ways analogous to photons in classical geometrical optics. Ohmic contacts act as electron sources and electron absorbers (Spector *et al* 1990a). Regions totally depleted of 2D electrons such as mesa edges and under highly biased gates act as almost perfect electron reflectors (Spector *et al* 1990a). Partially depleted regions refract electrons in accordance with an equivalent of Snell's law in optics (Spector *et al* 1990b). Beams of 2D ballistic electrons can be created and they are able to intersect each other with negligible interaction (Spector *et al* 1991). Using these novel control elements we demonstrate a 2D electron lens that focuses electrons from a point source onto a point detector by means of a photolithographically defined electrostatic lens of variable "index of refraction" (Spector *et al* 1990b). In a similar arrangement, an electrostatic prism can steer a beam of ballistic electrons onto three spatially separated electron detectors (Spector *et al* 1990c). High-mobility, two-dimensional electron systems, combined with modern lithographic techniques, lend themselves at low temperatures to the implementation of a wide variety of control elements that closely resemble the devices portrayed in textbooks on geometrical optics.

References

Pfeiffer L N, West K W, Stormer H L, Baldwin K W 1989 *Appl. Phys. Lett.* **55** 1880
Spector J, Stormer H L, Baldwin K W, Pfeiffer L N, West K W 1990a *Appl. Phys. Lett.* **56** 967
Spector J, *et al* 1990b *Appl. Phys. Lett.* **56** 1290
Spector J, *et al* 1991 *Appl. Phys. Lett.* **56** 263
Spector J, *et al* 1990c *Appl. Phys. Lett.* **56** 2433

* Present address: Arizona State University, Tempe, Arizona 85287

Taylor & Francis
Taylor & Francis Group
http://taylorandfrancis.com

Inst. Phys. Conf. Ser. No 120: Chapter 2
Paper presented at Int. Symp. GaAs and Related Compounds, Seattle, 1991

Facet formation observed in MOMBE of GaAs on a patterned substrate

Y.MORISHITA, Y.NOMURA, S.GOTO, Y.KATAYAMA, and T.ISU*

Optoelectronics Technology Research Laboratory,
5-5 Tohkodai, Tsukuba, Ibaraki 300-26, Japan

**Central Research Laboratory, Mitsubishi Electric Corporation,*
8-1-1 Tsukaguchi-Honmachi, Amagasaki, Hyogo 661, Japan

Abstract A detailed investigation was carried out on facet formation in the metalorganic molecular beam epitaxy (MOMBE) of GaAs on a mesa-etched (100) GaAs substrate by in situ scanning microprobe reflection high-energy electron diffraction (μ-RHEED) in real time. The distribution of the growth rates on the (100) surface near the edge of the mesa-groove was also measured by μ-RHEED. Besides the initial (100) surface and a (111)A sidewall, a (411)A facet as well as (311)A and ($5\bar{1}1$)A facets were formed at the lower and upper sidewalls, respectively, at growth temperatures between 540 and 620 °C. It was found that the formation of the ($5\bar{1}1$)A and (411)A facets is substantially associated with the exponential variation of the growth rate on the (100) surface, due to the flow of either Ga adatoms or Ga compounds from the sidewall to the (100) surface of the mesa pattern.

1. Introduction

Epitaxial growth on patterned substrates is useful for achieving advanced structures of optoelectronic devices such as laser diodes (Dzurko et al. 1989), waveguides (Colas et al. 1989), and transistors (Asai et al. 1984). For these devices, it is important to control the shapes of the epitaxial layers, especially in the active region of the device. It is well known that crystal planes with different indices affect the growth behavior on neighboring surfaces in molecular beam epitaxy (MBE) and metalorganic chemical vapor deposition (MOCVD) on patterned substrates. It has been reported that facets are formed between different crystal planes during growth (Tsang and Cho 1977, Hersee et al. 1986).

There have been few theoretical studies so far on the fundamental growth morphology formed on patterned substrates; Wulff (Wulff 1901) has reported that an epitaxial layer tends to form a shape which minimizes the total surface energy of the crystals, and that the shape is determined by the orientation dependence of the surface energy. Jones et al. (Jones et al. 1991) have applied the Wulff constriction to the prediction of edge shapes for nonplanar epitaxial growth, and have shown that the shapes of epitaxial layers are basically predetermined by the Wulff construction replacing the energy polar diagram with a growth rate polar diagram. Ohtsuka and Suzuki (Ohtsuka and Suzuki 1989) have

simulated GaAs growth on patterned substrates using a model which takes into account the effects of the incorporation, desorption and surface migration of Ga adatoms, and have demonstrated that, by assuming a certain migration length, bump-like shapes are formed on epitaxial layers grown on convex surfaces.

Although metalorganic molecular beam epitaxy (MOMBE) is a promising growth technique, the growth mechanism is still under intense investigation. We (Morishita et al. 1991) have observed facet formation during the MOMBE of GaAs on a mesa-etched (100) GaAs surface by scanning microprobe reflection high-energy electron diffraction (μ-RHEED) in real time, and have shown that the shape of the growing surface can be exactly monitored by μ-RHEED.

In this paper, we report on a detailed investigation of the effects of the growth temperature on facet formation in the MOMBE of GaAs on a mesa-etched (100) GaAs surface by μ-RHEED in real time. We also discuss the influences of the variation of the growth rate measured on the (100) surface near the edge, due to surface migration of Ga adatoms or Ga compounds, upon the shapes of epitaxial layers.

2. Experimental

GaAs MOMBE growth was carried out on (100) substrates with mesa-grooves along the $[0\bar{1}1]$ direction having outward sloping sidewalls. Growth apparatus used in this study and substrate preparation were described elsewhere (Morishita et al. 1991). In the MOMBE growth, trimethylgallium (TMGa) was delivered through a low-temperature (100 °C) effusion cell. The flow rate of TMGa was controlled at 1.0 SCCM by an electronic mass flow controller. Arsenic was supplied as a molecular beam and the flux was 8×10^{-4} Pa on a beam flux monitor. The substrate temperatures (T_S) from 540 to 620 °C were monitored by an infrared pyrometer. The growth rate on the (100) surface far from the edge of a mesa-groove was about 0.4 μm/h.

For RHEED measurements, a 25 keV electron beam with a diameter of about several hundred Å was aligned along the $[0\bar{1}1]$ azimuth. Fig.1 shows a schematic illustration of the epitaxial layer. The upper drawings represent the RHEED patterns observed at each point between a and f in the lower figure. The incident electron beam scanned the surface around the sidewall along a line normal to the edge of the mesa-groove (namely, parallel to the $[0\bar{1}1]$ direction) at a speed of 16 sec/line. The observed RHEED patterns during growth were recorded in real time with a video system. In the present experiment, the electron beam scanned a width of about 135 Å during one frame of the video picture. The indices of the surfaces were determined from the angle of the RHEED patterns at each point on the scanned line. The widths of

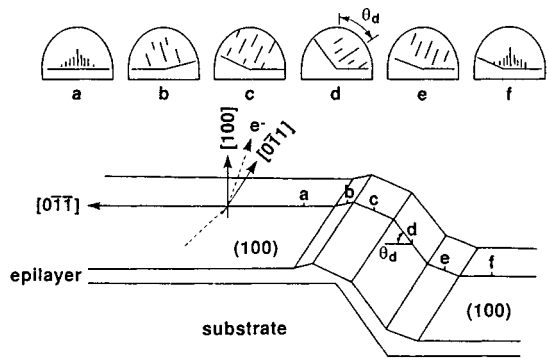

Fig. 1 Schematic diagram of the epitaxial layer. The upper drawings represent the RHEED patterns observed at each point between a and f in the lower figure.

the facets were estimatedfrom the number of video frames on which the RHEED patterns from the respective facets were taken during one scan.

The distribution of the growth rates on the (100) surface was measured from the periods of the RHEED intensity oscillation at each point on the scanned line. For growth rate measurements, the incident electron beam scanned the (100) surface near the edge of the mesa-groove along the [0 $\bar{1}$1] direction for 20 msec/line. Details of the measurement system have been described elsewhere (Isu et al. 1991). This technique is very useful in simultaneously obtaining the distribution of growth rates in an observed area within a few monolayer growth sequence.

3. Results

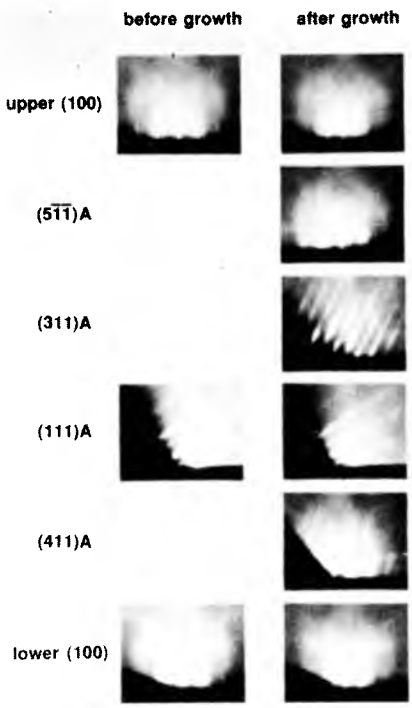

Fig. 2 Change of RHEED patterns observed at each point on the scanned line around a sidewall of a patterned substrate before and after growth.

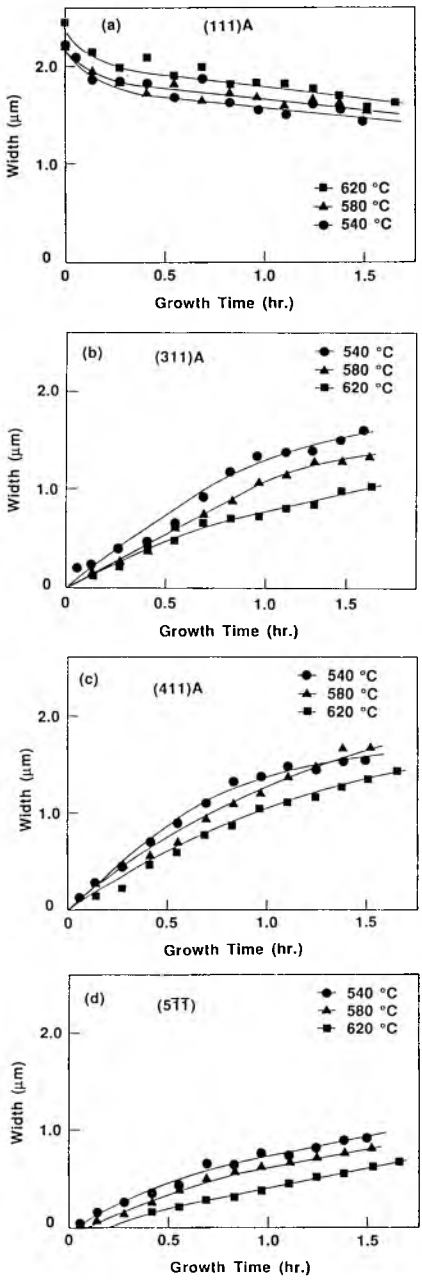

Fig. 3 The growth time dependence of the width of the (a) (111)A, (b) (311)A, (c) (411)A, and (d) (5$\bar{1}$1)A facet observed in MOMBE of GaAs for various growth temperatures.

Fig. 2 shows a set of RHEED patterns at each point on the scanned line around a sidewall of the patterned substrate before and after 1.5 hr growth at T_S of 580 °C. The RHEED patterns from a (100) surface and a sidewall with an intersecting angle of about 53° with the (100) plane were observed before growth, indicating that the initial face revealed on the sidewall was a (111)A plane. The onset of growth led to the appearance of RHEED patterns from new facets with different characteristic angles. The facet appearing at the lower sidewall had an intersecting angle of about 20° with the (100) plane; two facets at the upper sidewall had intersecting angles of about 25° and 15° with the (100) plane, respectively. These new facets appearing at the upper sidewall intersected each other at an angle of about 140°. Almost exactly the same tendency was observed with the RHEED patterns from the epilayers grown at T_S between 540 and 620 °C, indicating that the facets with the same indices are formed at the lower and upper sidewalls, respectively, under the experimental conditions studied. The facets with intersecting angles of about 20, 25, and 15° with the (100) surface correspond to the (411)A, (311)A, and $(5\bar{1}1)$A planes, respectively.

The widths of each facet observed in MOMBE of GaAs are plotted in fig. 3 for various growth temperatures as a function of the growth time. For all of the growth temperatures, the RHEED patterns from the (411)A and (311)A facets were observed immediately after the start of growth. Their width increased rapidly with growth up to about 1 h, and slightly thereafter. On the other hand, the width of the (111)A sidewall decreased rapidly with growth; the tendency then slowed down slightly. The gradient of the variation of the width for all facets increased as the growth temperature was lowered. These results indicate that (411)A and (311)A facets are quickly formed on the intersection regions between the initial (100) surface and the (111)A sidewall after the start of growth, and that the rapid development for the first 1 h of growth is enhanced at lower growth temperatures. At all growth temperatures, unlike in other cases involving different facets, the RHEED pattern from the $(5\bar{1}1)$A facet appeared after about 0.2 h of growth; the onset of the appearance increased from about 0.05 to 0.25 h as the growth temperature was raised from 540 to 620 °C. The width increased asymptotically as growth proceeded. These results suggest that a different factor affects the formation of the $(5\bar{1}1)$A facet. Details are discussed in the next section.

A set of $(01\bar{1})$ cross-sectional drawings of the epitaxial layers after 1.5 h growth which are determined by the width of each facet is shown in fig. 4. The contours of the epitaxial layers determined using μ-RHEED agree well with those obtained from secondary electron microscope observations at all growth temperatures.

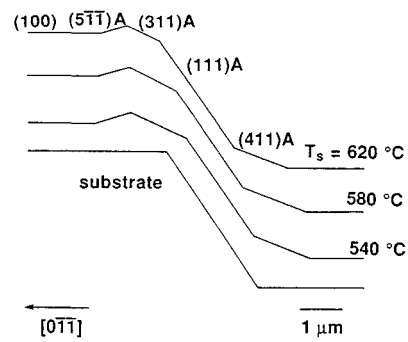

Fig. 4 A $(01\bar{1})$ cross-sectional drawing of the epitaxial layers grown at different growth temperatures.

4. Discussion

In order to explain the shapes of the epitaxial layers, we measured the growth rates on the planar (100), (111)A, (311)A, (411)A, and (511)A substrates at T_S between 540 and 620 °C. The growth rates were measured from the thicknesses of the epitaxial layers grown simultaneously on the same substrate holder. The results are summarized in table 1 for various growth temperatures. The growth rates for the (100) substrate were exactly equal to those obtained from the periods of the RHEED intensity oscillation on the (100) surface far from the edge of a mesa-groove of the patterned

Table 1. Growth rates on each substrate for various growth temperatures.

T_S (°C)	growth rate (μm/hr)				
	(100)	(111)A	(311)A	(411)A	(511)A
540	0.40	0.35	0.27	0.37	0.42
580	0.40	0.25	0.32	0.41	0.50
620	0.43	0.10	0.35	0.44	0.53

substrate at all growth temperatures. The growth rates on the (100), (311)A, (411)A, and (511)A substrates increased with raising growth temperature. On the other hand, the value for the (111)A substrate decreased as the growth temperature was raised. As has been proposed by Jones et al. (Jones et al. 1991), using the values of the growth rates summarized in table 1, the contours of the epitaxial layers are predicted for various growth temperatures by a Wulff construction, replacing the energy polar diagram with a growth rate polar diagram. The results are shown in fig. 5 for different growth temperatures.

On the other hand, the growth rate on the (100) surface near the edge of the mesa-groove was reported to vary exponentially as a function of the distance from the edge during MBE of GaAs, due to the flow of Ga adatoms from the (111)A sidewall to the (100) surface of the mesa pattern (Hata et al. 1990). The growth rates on the (100) surface near the edge were measured using the same technique during the MOMBE of GaAs. The exponential dependence of the increase of the growth rate on the distance from the edge was also obtained for the MOMBE of GaAs. In order to take into account the effect of the flow of Ga adatoms or Ga compounds from the (111)A sidewall to the (100) surface, the shapes of the epitaxial layers were modified by adding the increase of growth rates on the (100) surface near the edge of a mesa-groove to those on the planar (100) substrate. The results are also drawn in fig. 5. The lowermost and uppermost lines at each growth temperature represent the drawing of the substrate before growth and that of the contour of the epitaxial

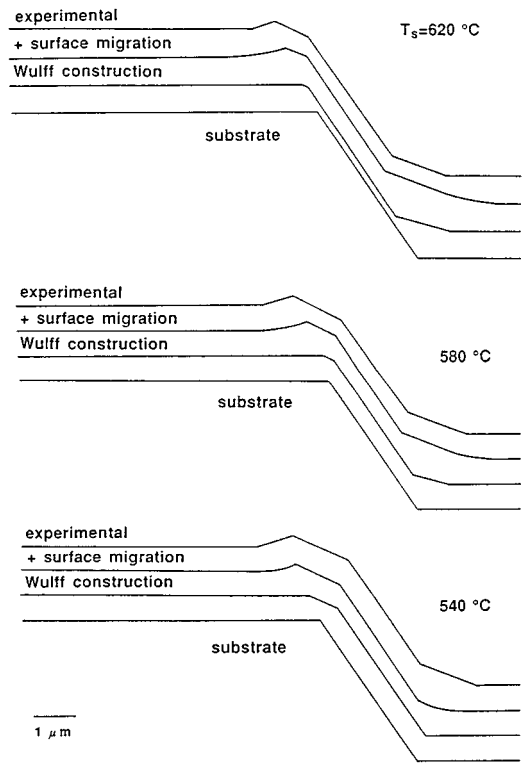

Fig. 5 A $(01\bar{1})$cross-sectional view of the epitaxial layers obtained using μ-RHEED observations and those determined by the Wulff constructions with and without taking into account the flow of Ga adatoms or Ga compounds.

layer obtained using μ-RHEED, lrespectively.

The result clearly indicates that the bump-like shape comprising of the (5$\bar{1}$1)A and (311)A facets is only obtained by taking into account
the flow of Ga adatoms or Ga compounds. On the intersection region between the (100) surface and the lower (111)A sidewall, the Wulff construction predicts no facet at T_S=540 °C; a (511)A facet is predicted at T_S>580 °C. However, the (411)A facet is actually observed by μ-RHEED. The formation of the (411)A facet is also considered to be due to the flow of Ga adatoms or Ga compounds from the (111)A sidewall to the lower (100) surface. In other words, it is considered that the surface migration of adatoms affects the formation of the (411)A facet. Although it is very difficult to measure the distribution of the growth rates on each facet, investigations about the surface migration on the facet are desired in order to exactly understand the shapes of the epitaxial layers.

5. Conclusion

A detailed observation was carried out on facet formation during the MOMBE of GaAs by μ-RHEED in real time. The distribution of the growth rates on the (100) surface near the edge of a mesa-groove was also measured by μ-RHEED. Besides the initial (100) surface and (111)A sidewall, a (411)A facet and (311)A and (5$\bar{1}$1)A facets were formed at the lower and upper sidewalls, respectively, at growth temperatures between 540 and 620 °C. It was found that the formation of (5$\bar{1}$1)A and (411)A facets is substantiality associated with the exponential variation of the growth rate on the (100) surface, due to the flow of Ga adatoms or Ga compounds from the sidewall to the (100) surface of the mesa pattern.

Acknowledgment

The authors would like to thank Dr. I.Hayashi for enlightening discussions and continuous encouragement.

References

Asai H, Adachi S, Ando S, and Oe K 1984 J. Appl Phys. 55 3868.
Colas E, Yi-Yan A, Bhat R, Seto M, and Deri R 1989 Appl. Phys. Lett. 54 1501.
Dzurko K M, Menu E P, Beyler C A, Osinski J S, and Dapkus P D 1989 Appl. Phys. Lett. 54 105.
Hata M, Isu T, Watanabe A, and Katayama Y 1990 Appl. Phys. Lett. 56 2542.
Hersee S D, Barbier E, and Blondeau R 1986 J. Crystal Growth 77 310.
Isu T, Hata M, Morishita Y, Nomura Y, and Katayama Y 1991 to be published in J. Crystal Growth.
Jones S H, Seidel L K, Lau K M, and Harold M 1991 J. Crystal Growth 108 73.
Morishita Y, Nomura Y, Goto S, Katayama Y, and Isu T 1991 to be published in Surface Sci.
Ohtsuka M and Suzuki A 1989 J. Crystal Growth 95 55.
Tsang W T and Cho A T 1977 Appl. Phys. Lett. 30 293.
Wulff G 1901 Z. Krist. 34 449.

Inst. Phys. Conf. Ser. No 120: Chapter 2
Paper presented at Int. Symp. GaAs and Related Compounds, Seattle, 1991

Atomically flat AlGaAs/GaAs (110) heterointerface grown by molecular beam epitaxy

G.Tanaka, K.Hirakawa, H.Ichinose and T.Ikoma

Institute of Industrial Science, University of Tokyo,
7-22-1 Roppongi, Minato-ku, Tokyo 106, Japan

Abstract : We found that one of the difficulties in growing (110) AlGaAs/GaAs hetero-structures with a high-quality interface is the lack of steps to stabilize Ga atom migration during growth. Insertion of an InAs buffer layer introduces a high density of misfit dislocations which provide equivalent steps at the growing surface. We found, however, that the hetero-interface of the structures grown by this method is very poor and neither quantum wells nor modulation doped hetero-interfaces can be grown.

We have shown that by lowering the growth temperature down to 400°C and using a high As_4 to Ga ratio (30), atomically flat (110) interface can be obtained. The FWHMs of photo luminescence spectra from quantum wells with different well widths are as narrow as those of the best (100) hetero-interface and the fluctuation of the interface roughness is less than one monolayer.

Introduction

High-quality AlGaAs/GaAs quantum wells and superlattices have been successfully grown on (100) substrates and a relatively flat hetero-interface with one mono-layer fluctuations has been obtained. At a (100) surface, anion and cation atoms sit on slightly different planes and therefore dipoles are possibly formed at the hetero-interface. The interface dipoles can contribute to the band discontinuity, which has been a hot topic discussed by many authors (Capasso et al 1985, Waldrop et al 1990, Lambrecht et al 1990, Peressi et al 1991, Sorba et al 1991).

On the other hand, at a (110) surface, anion and cation atoms sit on the same plane and the charge neutrality holds in the plane (Harrison et al 1978). Therefore, we expect no interface dipole layer to be formed (homopolar interface), and a very flat interface should be obtained on this crystal plane. However, so far only a few (Munekata et al 1987, Allen et al 1987, Zhou et al 1987) high quality interfaces have been reported on the (110) growth surface. Thus, it is important and interesting to determine the optimal growth condition to obtain a high quality (110) interface from the view point of practical applications as well as investigating the effects of interface dipoles on the hetero-interface band offset.

Munekata et al. reported that when a thin InAs layer was inserted between the substrate and an epitaxial layer, a mirror like surface was obtained on a (110) substrate. They did not, however, report the quality of the interface. Allen et al. reported that a hetero-structure with a mirror like surface was obtained on a (110) substrate tilted by 6° toward $(1\bar{1}1)$ at temperatures higher than 550°C. On the other hand, Zhou et al. succeeded in growing a hetero-structure with relatively high electron mobility on an untilted (110) substrate when the growth temperature is low (470-500°C) and the As_4 to Ga ratio is high (20-30).

In this paper, we first test the method of Munekata et al. stressing the characterization of the hetero-interface. Secondly, we determine an optimal condition to grow AlGaAs/GaAs hetero-structures on an untilted (110) substrate without an InAs layer, in

order to obtain a high quality interface. Finally, we characterized those interfaces by photoluminescence and the mobility of two dimensional electron gas.

Role of InAs buffer layer

We simultaneously grew AlGaAs/GaAs single hetero-structures on untilted (100) GaAs substrates with and without a thin InAs buffer layer by molecular beam epitaxy (MBE). The growth temperature was varied from 400°C to 600°C, and As_4 to Ga ratio from 5 to 35. The composition of Al in AlGaAs is 0.3. The surface morphologies were observed with an optical microscope and an atomic force microscope (AFM) shown in Fig. 1(a). We confirmed that the insertion of a thin InAs layer could improve surface morphologies as shown in Fig.1 (b) and (c) as reported by Munekata et al.

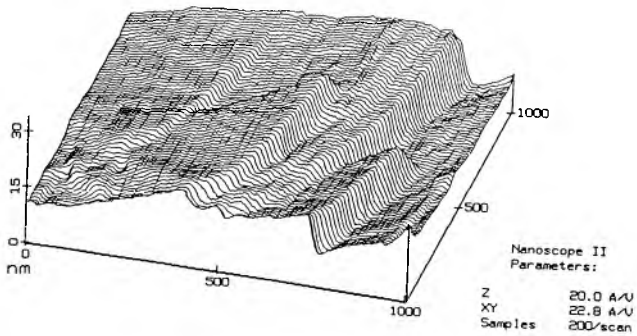

Figure 1(a) AFM image of fasets on surface.

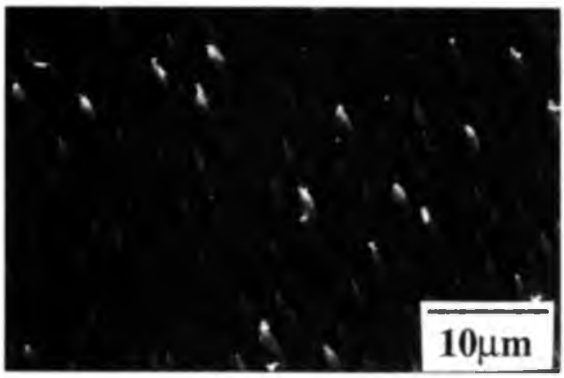

Figure 1(b) SEM image of surface morphology grown without an InAs buffer layer. Many facets are observed on surface.

Figure 1(c) SEM image of surface morphology grown with an InAs buffer layer. By comparison with (a), a facet growth is suppressed by inserting an InAs buffer layer and a mirror-like surface is obtained.

In order to investigate the interface flatness, we fabricated quantum wells with various well widths as shown in Fig.2 and measured the photoluminescence at 77K. No clear exciton lines were observed as shown in Fig.3. There is a broad peak around 720 nm, suggesting that at the interfaces AlGaAs and GaAs were mixed and formed an alloy. The electron mobility at 77K was also very low (3000 cm^2/Vs). This indicates that the insertion of an InAs buffer layer is not a suitable method to obtain a high quality (110) interface.

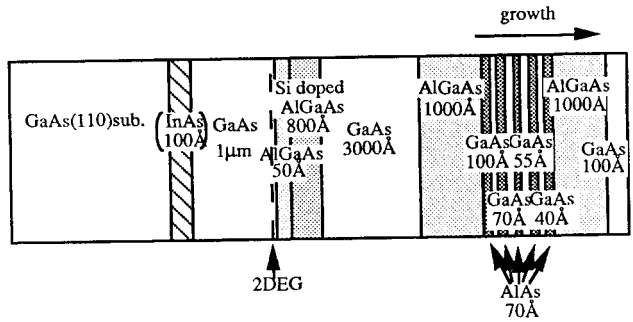

Figure 2 Quantum wells grown for characterization of interfaces

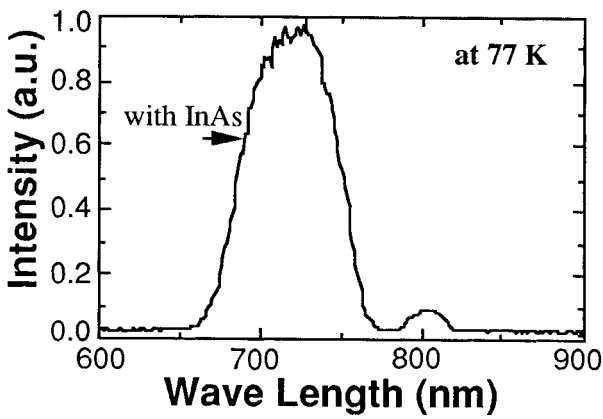

Figure 3 Photoluminescence spectrum from quantum wells at 77 K. The growth temperature is 450°C. No peaks from quantum wells are obserbed. There is a broad peak which suggests that no well-defined quantum wells are formed.

The scanning electron microscope images of cleaved surfaces of the two wafers grown under the same condition on (110) and (100) substrates are shown in Fig.4 (a) and (b). Apparently, the growth rate on (110) substrates is 0.8 times smaller than that on (100) substrates. This shows that the sticking probability of Ga atoms is lower on (110) surface than on (100) surface. This fact leads us to speculate that Ga atoms migrate for longer distance on a (110) surface than on a (100) surface to find stable positions before they stick on steps or kinks on the surface and thus have a larger probability to re-evaporate from the surface. This is reasonable since (110) surface has less steps. Moreover, a transmission electron microscope lattice image was taken on the cleaved surface (a cross sectional image) of the (110) AlGaAs/GaAs hetero-structure with an InAs buffer layer and is shown in Fig.5. As shown in the figure many dislocations are generated due to large mismatch of the lattice constants. These dislocations play an important role in providing equivalent steps where Ga atoms can stick stably before they re-evaporate. Thus, an apparent two-dimensional growth becomes possible by insertion of an InAs layer. This growth condition is similar to the case of highly misoriented substrates (Allen et al 1987), which have many steps at the surface. However, it is easily seen that such heterostructures formed with the InAs layer will give poor electronic and optical properties which was confirmed through the photoluminescence spectra and electron mobility.

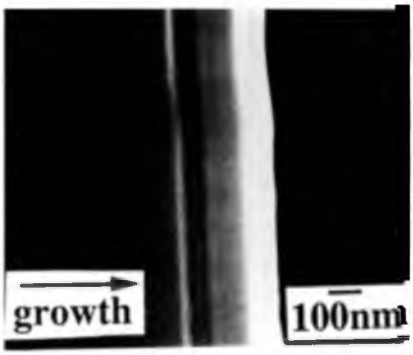

Figure 4(a) SEM image of a cleaved surface grown on a (100) substrate. The white areas are AlGaAs layer. The black areas are GaAs layer.

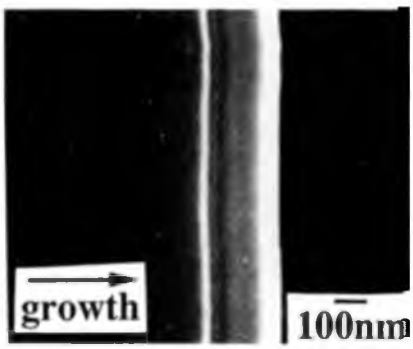

Figure 4(b) SEM image of a cleaved surface grown on a (110) substrate. Comparing with (a), GaAs layers are thinner, showing that Ga atoms are likely to re-evaporate on a (110) surface.

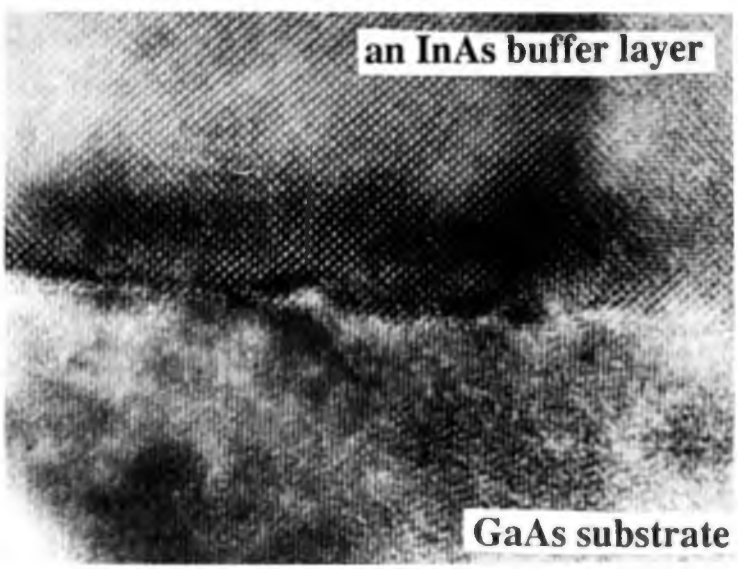

Figure 5 TEM image of the interface between GaAs(110) substrate and an InAs buffer layer. At the interface many dislocations are introduced by large mismatch of lattice constance. These dislocations tilt the growth plane.

Optimal Growth Condition

From the above observations we find that one of the difficulties of growing thin (110) epitaxial layers is due to the fact that Ga atoms migrate very long distance and re-evaporate before sticking at steps or kinks on the surface. Therefore it is desirable to set up the growth condition in such a way as to suppress Ga atom migration and re-evaporation. One of the means to do so is to provide steps or kinks by introducing a strained buffer layer or by using misoriented surfaces as mentioned in the previous section. However these methods do not give a high-quality interface which is a goal of the present investigation. Another means is to lower the growth temperature to reduce the surface migration, and to increase the As_4 to Ga ratio to suppress re-evaporation of Ga atoms.

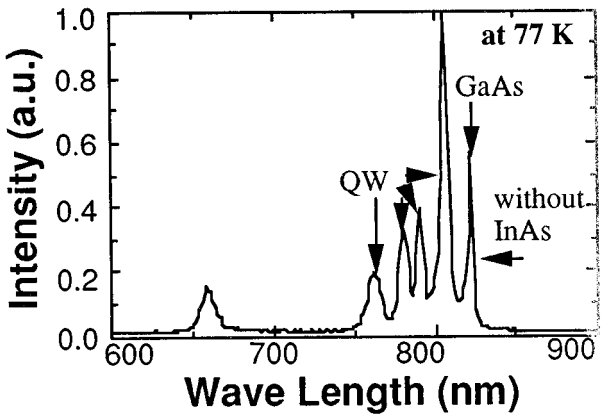

Figure 6 Photoluminescence spectrum from quantum wells at 77 K. Without an InAs buffer layer, the peaks from quantum wells are apparently obserbed.

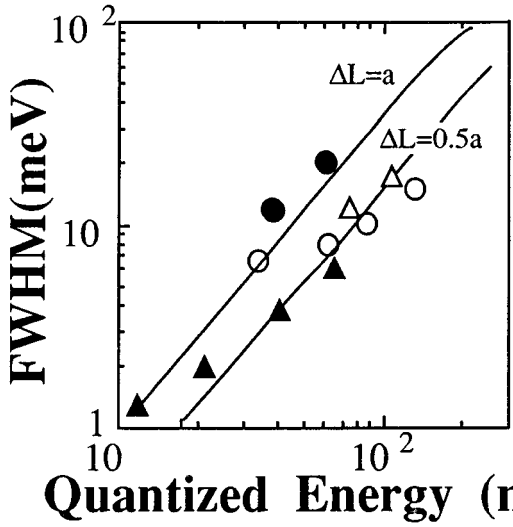

	growth temp.	V/III ratio	substrate
○	400°C	35	(110)
△	400°C	35	(100)
●	500°C	35	(110)
▲	600°C	5	(100) a)

a) C. Weisbush et al. 1981

Figure 7 FWHM of photoluminescence spectra as a function of quantized energy. Theoretical curves are obtained by assuming that fluctuations of the interface roughness are one to a half monolayer.

We grew (110) AlGaAs/GaAs quantum wells, which are schematically shown in Fig. 2, and modulation-doped single hetero-structures, in which the electron density is 5×10^{-11} cm^{-2}, at growth temperature of 400°C and an As_4 to Ga ratio of 30. The Al composition in the AlGaAs layers is 0.3.

The surfaces of these structures are all mirror like. The photoluminescence spectrum is shown in Fig.6, which shows clear excitonic peaks corresponding to each quantum well. As usual we plotted the full width at half maximum (FWHM) as a function of quantized energy in Fig.7 with growth temperature as a parameter. The FWHM is as narrow as that from one of the best (100) quantum wells (Weisbush et al 1981) and falls between the two theoretical curves which assume interface fluctuations of one-half to one monolayer as shown in the figure. The mobility of two dimensional gas was 60000 cm^2/Vs at 77K, which is comparable to that at (100) interface.

Thus, we obtained high quality hetero-interface on untilted (110) GaAs substrates without the use of an InAs layer at a low substrate temperature of 400°C and a high As_4 to Ga ratio of 30.

Conclusions

We found that one of the difficulties in growing (110) AlGaAs/GaAs hetero-structures with a high-quality interface is the lack of steps to stabilize Ga atom migration during growth. Insertion of an InAs buffer layer (Munekata et al 1987) introduces a high density of misfit dislocations which provide equivalent steps at the growing surface. We found, however, that the hetero-interface of structures grown by this method is very poor and neither quantum wells nor modulation doped hetero-interfaces can be grown.

We have shown that by the lowering growth temperature down to 400°C and using a high As_4 to Ga ratio (30), atomically flat (110) interface can be obtained. The FWHMs of quantum wells with different well widths are as narrow as those of the best (100) hetero-interface and the fluctuation of the interface roughness is less than one monolayer. These optimal conditions are similar to those of Zhou et al. but the growth temperature is smaller than theirs.

Acknowledgements

The authors wish to express their sincere thanks to T. Saito, Y. Hashimoto and M. Noguchi for discussions. We also thanks to S. Ozawa of Furukawa Electric Co. for supplying us the GaAs substrates. This work is supported by the Grant-in-Aid from the Ministry of Education, Science, and Culture, Japan, by the Foundation of Promotion of Material Science and Technology of Japan (MST), and also by the Industry-University Joint Research Program "Mesoscopic Electronics."

References

Allen L T P, Weber E R, Washburn J, and Pao Y C, Appl. Phys. Lett. **51**, 670 (1987).
Capasso F, Cho A Y, Mohammed K, and Foy P W, Appl. Phys. Lett. **46**, 664 (1985).
Harrison W A, Kraut E A, Waldrop J R, and Grant R W, Phys. Rev. B **18**, 4402 (1978).
Lambrecht W R L, Segall B, and Andersen O K, Phys. Rev. B **41**, 2813 (1990).
Munekata H, Chang L L, Woronick S C, and Kao Y H, J. of Crystal Growth **81**, 237 (1987).
Peressi M, Baroni S, Resta R, and Baldereschi A, Phys. Rev. B **43**, 7347 (1991).
Sorba L, Ceccone G, Antonini A, Walker J F, Micovic M, and Franciosi A, Phys. Rev. B **43**, 2450 (1991).
Waldrop J R, Kraut E A, Farley C W, and Grant R W, J. Vac. Sci. Technol. B **8**, 768 (1990).
Weisbuch C, Dingle R, Grossard A C, Wiegmann W, Solid State Commun. **38**, 709 (1981).
Zhou Junming, Huang Yi, Li Yongkang, and Jia Wei Yi, J. of Crystal Growth **81**, 221 (1987).

Inst. Phys. Conf. Ser. No 120: Chapter 2
Paper presented at Int. Symp. GaAs and Related Compounds, Seattle, 1991

Abrupt heterojunctions of AlGaAs/GaAs quantum wells grown on (111)A GaAs substrates by molecular beam epitaxy

T. Yamamoto, M. Fujii, T. Takebe, D. Lovell, and K. Kobayashi

ATR Optical and Radio Communications Research Laboratories, Seika-cho, Soraku-gun, Kyoto 619-02, Japan

ABSTRACT

Morphologies and interface abruptness of AlGaAs/GaAs on (111)A GaAs substrates are studied using single quantum well (SQW) structures consisting of five GaAs layers of variable thickness. They are grown on exactly (111)A GaAs and (111)A GaAs surfaces that are misoriented towards the [100] direction by 1°, 3°, and 5°. The abruptness of AlGaAs/GaAs heterojunctions grown on GaAs (111)A surfaces has been evaluated by photoluminescence(PL) intensity measurements. It has been demonstrated that the PL peak wavelengths for SQW structures on the exactly and 5°- misoriented (111)A surfaces agree with the values calculated with the effective mass of the heavy hole of $m^*_{hh}=0.9m_0$. The abruptness of SQW structures on these surfaces is estimated as less than one monolayer from full width at half maximum(FWHM) values.

1. Introduction

Recently, epitaxial growth on patterned substrates has stimulated interest in the fabrication of lateral microstructures (Miller, Meier et al, and Kapon et al 1985, 1987, and 1987). The differences in doping type, layer thickness, and composition of ternary alloy systems between the slope and the flat are main topics of interest. With regard to epitaxial growth on (100) substrates patterned with one-dimensional features, advanced devices with lateral carrier confinement structures, such as quantum wire lasers, have attracted much attention (Kapon et al 1990). Three-dimensional confinement of carriers, such as quantum dots, may be obtained similarly by molecular beam epitaxial (MBE) growth on substrates patterned with two-dimensional features. We have made good use of the threefold rotational symmetry of the (111)A surface, and obtained an equilateral triangle pattern in which three slopes have equivalent crystallographic faces. The conductivity type of MBE grown Si-doped GaAs layers on (111)A-oriented GaAs is controlled by the growth conditions and the degree of (111)A substrate misorientation towards the (100) surface (Okano et al 1990). We have proposed and realized a new type of carrier confinement structure by the combination of these interesting properties (Fujii et al 1991).

However, it is difficult to grow GaAs and AlGaAs layers that have good surface morphology on the (111)A GaAs. Our purpose is to solve the above problem and to achieve a surface morphology and heterointerface that is satisfactory for fabricating optical devices. It has been reported that the morphology of GaAs and AlGaAs layers on (111)A substrates are dependent on growth conditions (Fuke et al 1990) and misorientation angle (Okano et al 1990). Recently, we have found that the morphology of GaAs and AlGaAs layers on (111)A substrates are strongly dependent on surface treatment conditions for the GaAs substrates before the growths (Yamamoto et al 1991).

In this paper, we investigate the dependence of the surface morphology and heterointerface quality of MBE AlGaAs/GaAs single quantum wells on (111)A GaAs substrates, upon the surface misorientation under optimized surface treatment conditions, in order to obtain mirror-like surface and high quality in epitaxial layers.

2. Experiment

Samples under study were grown by MBE on semi-insulating exactly (111)A oriented GaAs wafers and those 1°-, 3°- and 5°- misoriented towards [100]. The substrates were cleaned by organic solvents and the surface native oxide layers were removed by $HCl:H_2O$. Then, they were etched in $NH_4OH:H_2O_2:H_2O$ solution and rinsed in de-ionized (DI) water. The above etchant was intentionally selected because the etch rate is very low and it leaves a smooth surface. The thermal etching temperature was 780 °C under a As_4 flux intensity of $3.2x10^{-5}$ Torr. (We have purposed the optimized surface treatments for (111)A substrates (Yamamoto et al 1991). The good surface morphology have been obtained on condition that higher thermal etching temperature under higher As_4 flux intensity than those of (100).) The temperature of $Al_{0.5}Ga_{0.5}As$/GaAs SQWs growth was kept at 600 °C . The As_4/Ga flux ratios (γ) were about 7.5 for GaAs and 5.0 for $Al_{0.5}Ga_{0.5}As$, respectively. The growth rates, corrected by reflection high energy electron diffraction (RHEED) oscillations, were about 1.0μm/h for $Al_{0.5}Ga_{0.5}As$ and 0.5μm/h for GaAs. First, a GaAs buffer layer (0.2nm) and an $Al_{0.5}Ga_{0.5}As$ barrier layer (50nm) were grown on (111)A GaAs substrates. Then, a SQW structure consisting of five GaAs layers of varying thickness, 2, 3, 5, 9, and 13nm, each separated by an 50nm $Al_{0.5}Ga_{0.5}As$ layer, was grown. In order to investigate the dependence of optical properties on the tilt angle, all the (111)A substrates and an (100) substrate were placed side by side on a substrate holder. No growth interruption was done between the wells(GaAs) and the barriers(AlGaAs). Surface morphologies were observed by scanning electron microscopy(SEM). Photoluminescence(PL) spectra were measured at 15K using the 488nm line of an Ar ion laser.

3. Results and Discussion

Figure 1(a), (b), (c), (d), and (e) show photoluminescence spectra of SQWs on the exactly (111)A GaAs wafer, those 1°-, 3°-, 5°- misoriented, and the (100) wafer with the five quantum wells, respectively. The PL peak wavelengths of all the (111)A SQWs are longer than those of the (100) SQWs. As the misorientation from (111)A increases, the PL peaks show red shifts and the linewidths become broad. Unknown PL peaks appear in the high energy side for the (111)A 1°- and 3°- misoriented samples. The PL linewidth of the 5°-misoriented samples recover those of the exactly (111)A sample.

The peak wavelengths of PL spectra as a function of single quantum well width are shown in Fig. 2. The experimental transition wavelengths of the PL peaks are compared with theoretical values. The solid and broken lines are the calculations for (100) and (111)A orientations, respectively. It has been assumed that the recombination transition takes place between an electron and a heavy hole in the lowest eigenstates in a finite square potential well. The equation and band parameters used in the calculation

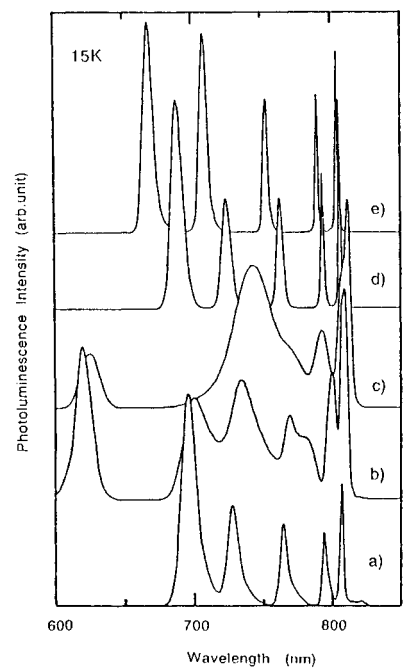

FIG. 1 PL spectra at 15K of the exactly (111)A oriented (a), 1°-, 3°-, and 5°- misoriented (111)A (b), (c), and (d), and the (100) SQWs (e). The dependence of PL peak wavelengths of AlGaAs/GaAs single quantum wells on the (111)A GaAs substrates upon the surface misorientation are shown.

Table I. The equation and band parameters used in the calculation.

Equation : $$tan\left(\sqrt{\frac{m_w E L_z^2}{2\hbar^2}}\right) = \frac{m_b (V - E)}{m_w E}$$

E: eigenvalue in the 1D finite square potential well, m_b, m_ω: barrier and well mass of the particle
L_z: well width, V: barrier height

Band parameters $m_0=9.11\times10^{-28}$ g, $E_g(T)=1.519-5.405\times10^{-4}T^2/(204+T)$

$V_c=0.63[1.247x+1.147(x-0.45)^2]$, $V_v=0.37[1.247x+1.147(x-0.45)^2]$

$m^*_{hh}GaAs[100]=(0.34)m_0$, $m^*_{hh}Al_xGa_{1-x}As[100]=(0.34+0.41x)m_0$

$m^*_{hh}GaAs[111]=(0.90)m_0$, $m^*_{hh}Al_xGa_{1-x}As[111]=(0.90+0.41x)m_0$

$m^*_eGaAs(E)=(0.0665+0.0436E+0.236E^2-0.143E^3)m_0$ (E in eV), $m^*_eAl_xGa_{1-x}As=(0.0665+0.083x)m_0$.

are listed in Table I.

The effective mass of the heavy hole for the (111) orientation is taken to be $m^*_{hh}Al_xGa_{1-x}As[111] = (0.90+0.41x)m_0$ (Hayakawa et al 1988). The dependence of the binding energy of two-dimensional electron-heavy-hole free excitons upon the quantum well width is taken into account in the calculation; 11 and 8 meV for well thicknesses of 4.2 and 14.5nm, respectively (Miller et al 1981). The valence-band discontinuity between GaAs and $Al_xGa_{1-x}As$ is taken to be 37% of the total band-gap differences ($\Delta Eg=1.247x+ 1.147(x-.45)^2$ (Casey et al 1978), assumed to be independent of temperature.

The PL peak wavelengths for every well width for the (100) SQWs are in good agreement with the solid line theoretically derived for the (100) orientation. This clearly shows that the desired SQW structures have been realized. The PL peak wavelengths for exactly and 5°- misoriented (111)A SQWs are consistent with the broken line theoretically derived for the (111) orientation. To our knowledge, this is first experimental demonstration that the effective mass of the heavy hole for the (111)A GaAs is $m^*_{hh}=(0.9)m_0$. On the other hands, the PL peak wavelengths for the 1°- and 3°- misoriented samples show red shift.

The dependence of the full width at half maximum (FWHM) upon the quantum

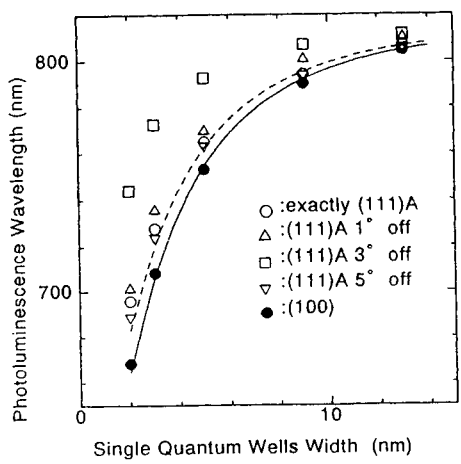

FIG. 2 Peak wavelengths of PL spectra as a function of single quantum wells width. The experimental transition wavelengths of the PL peaks are compared with theoretical values. The solid and broken lines are the calculations for (100) and (111)A orientations, respectively.

well width is shown in Fig. 3. The solid and broken lines are the theoretical FWHM values that are evaluated from $[\partial E^*/\partial L_z]dL_z$, E^* is the transition energy, assuming that the fluctuation of the well width (dL_z) is one monolayer for both (100) and (111)A orientation, respectively. For well width below 3nm, the FWHMs of (100), exactly (111)A and 5°- misoriented (111)A samples are narrower than the theoretical values. As a result, the abruptness of SQW structures on these surfaces can be estimated as less than one monolayer.

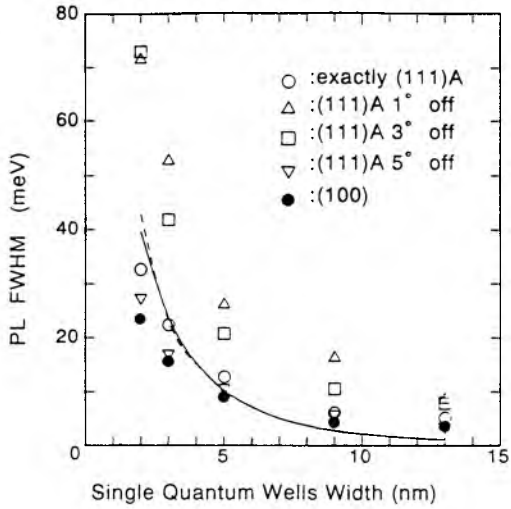

FIG. 3 Full width at half maximum (FWHM) as a function of the quantum well width. The solid and broken lines are the theoretical FWHM values which were evaluated from $[\partial E^*/\partial L_z]dL_z$, E^* is the transition energy, assuming that the fluctuation of the well width (dLz) is one monolayer for both (100) and (111)A orientations at 0K.

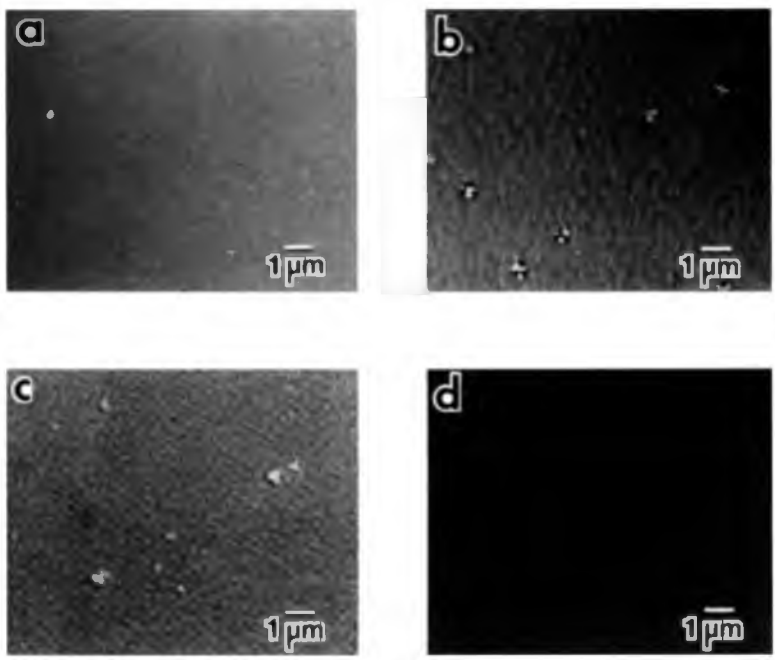

FIG.4 Surface morphology of the AlGaAs/GaAs SQW structures grown on the exactly (111)A GaAs (a), and 1°(b), 3°(c), and 5°(d)-misoriented toward [100]. The exactly (111)A surface exhibits a few defects and the 5° misoriented surface exhibits fewer defects. On the other hands, numerous giant steps and diamond shape terraces of submicron sizes are observed on the 1°- and 3°- misoriented surfaces.

Surface morphology of the AlGaAs/GaAs SQW structures grown on the exactly (111)A and 1°–, 3°–, and 5°–misoriented (111)A surfaces are shown in Fig. 4(a), (b), (c), and (d), respectively. The exactly (111)A surface exhibits a few defects and the 5°– misoriented surface exhibits fewer defects. On the other hand, numerous giant steps of submicron sizes are observed on the 1°– and 3°– misoriented surfaces. The red shift and broadening seen in the PL spectra are probably caused by these giant steps. The mechanism of giant step formation has been explained as follows: the growth processes consist of surface migration of the growth elements and subsequent quasi–equilibrium reactions at the kinks in the steps (Suzuki et al 1990).

4. Conclusion

We have also proposed a surface emitting laser using the new structure (Fujii et al 1991).

The abruptness of AlGaAs/GaAs heterojunctions formed on (111)A GaAs surfaces has been evaluated by photoluminescence for four types of MBE–grown samples which have five single quantum wells having well thicknesses, of 2, 3, 5, 9, and 13nm, respectively. The exactly (111)A surface exhibits a few defects and the 5°– misoriented surface exhibits fewer defects. The observed peak energies from these substrates agree well with the theoretical values, which are derived assuming that the effective mass of the heavy hole for the (111) orientation are $m^*_{hh}=(0.9)m_0$. The abruptness for SQW structures on these surfaces is estimated as less than one monolayer from FWHMs values. On the other hand, a red shift and broadening of the PL spectra, an appearance of a peak in the high energy side, and the giant steps are observed on the 1°– and 3°– misoriented surfaces. Thus, it seems that giant steps and diamond shape terraces observed only on these surfaces are responsible for the change in the PL spectra.

Acknowledgements

The authors would like to thank Dr. Y. Furuhama for his encouragement throughout this work. Thanks are also due to Dr. M. Shigeta for stimulating discussions.

References

Casey H.C. and Panish M. B. 1978, Heterostructure Lasers (Academic, New York, 1978),part A.

Fujii M., Yamamoto T., Shigeta M., Takebe T., Kobayashi K., Hiyamizu S., and Fujimoto I. 1991, The 5th International Conference on Modulated Semiconductor Structures (Nara, Japan, July 8–12,) pp.149–151

Fuke S., Umemura M., Yamada N., and Kuwahara K. 1990, J. Appl. Phys 68, 997

Hayakawa T., Takahashi K., Kondo M., Suyama T., Yamamoto S., and Hijikata T. 1988, Phys. Rev. Lett. 60 349

Kapon E., Tamargo M. C., and Hwang D. M., 1987, Appl. Phys. Lett. 50(6), 347

Kapon E., Simhony S., Harbison J. P., Florez L. T. and Worland P. 1990, Appl.Phys. Lett. 56, 1825

Meier H. P., van Gieson E., Broom R. F., Walter W., Webb D. J., Harder C. and Jäckel H., 1987, Int. Symp. GaAs and Related Compounds 1987, edited by A. Christou and H. S. Rupprecht (Institute of Physics, Bristol, 1988),pp.609–612

Miller D. L. 1985, Appl. Phys. Lett. 47 ,1309

Miller R. C., Kleinman D. A., Tsang W. T., and Gossard A. C. 1981, Rhys. Rev. B24, 1134

Okano Y., Shigeta M., Seto H., Katahama H., Nishine S., and Fujimoto I. 1990, Jpn. J. Appl. Phys. 29, L1357

Suzuki T. and Nishinaga T. 1990, The 9th Symp. Record of Alloy Semiconductor Physics and Electronics, Izu–Nagaoka 1990 July p187

Yamamoto T., Takebe T., Fujii M., and Kobayashi K. 1991, The 10th Symp. Record of Alloy Semiconductor Physics and Electronics, Nagoya 1991 July 18–19 p73

Inst. Phys. Conf. Ser. No 120: Chapter 2
Paper presented at Int. Symp. GaAs and Related Compounds, Seattle, 1991

Confinement of excess arsenic incorporated in thin layers of MBE-grown low-temperature GaAs

J.P.Ibbetson*, C.R.Bolognesi†, H.Weman‡, A.C.Gossard*†, U.K.Mishra†
Materials Dept.*, Dept. Electrical and Computer Engineering†,
QUEST Center for Science and Technology‡.
University of California, Santa Barbara, CA93106

Introduction

GaAs epilayers grown at low substrate temperatures (200-250°C) under otherwise normal MBE growth conditions are currently attracting much interest due to their unique electrical properties. Initially developed as buffer layers for power FET applications[1], Low-Temperature GaAs (LTGaAs) can reduce backgating in MESFETs [1]. Subsequently, surface layers of LTGaAs have also been employed to significantly improve MESFET gate-to-drain breakdown characteristics [2]. Most recently, indications of low-temperature (10K) superconductivity has also been reported in bulk LTGaAs [3], although this remains a controversial topic.

Material characterization studies have shown that the low growth temperature results in highly non-stoichiometric crystalline growth, with roughly 1 at.% excess As [4]. During annealing and/or postgrowth high temperature treatment the excess As redistributes itself in the crystal. In some cases metallic As precipitates have been observed [5].

Preventing out-diffusion of As-related defects into nearby active regions is very important for present and future applications of LTGaAs. Optical studies indicate that the presence of a LTGaAs buffer layer can significantly affect the quality of quantum wells ~1000Å away [6]. However, AlAs layers grown at normal growth temperatures (600°C) have been shown to prevent compensation of an n-type channel beneath LTGaAs surface layers [2]. In the present paper we present results on the optical properties of single and multiple quantum well structures incorporating thin layers (<150Å) of LTGaAs within barriers and well regions respectively. Photoluminescence (PL) is used to probe the quality of layers and interfaces in the immediate vicinity (~200Å) of LTGaAs layers,the optical properties of LTGaAs QW's, and the effectiveness of AlAs defect diffusion barriers.

MBE Growth

All samples in this study were grown in a Varian GENII solid source MBE system. Complete growth details will be published elsewhere [7]. All low-temperature (LT) growth was at a substrate temperature (T_{sub}) of 230°C as measured by a thermocouple. Otherwise growth occurred at T_{sub}=600°C.The growth rate was 0.5μm/hr, with an As_4:Ga beam equivalent pressure of 15:1.

Results

Two series of samples were grown. In the first series, a GaAs/AlGaAs single quantum well structure containing very thin layers of LTGaAs was studied. Bulk layers of LTGaAs have been shown to be optically dead, due to the large number of recombination centres they contain. In this study, the effect of these traps on the optical properties of thin layers of LTGaAs is determined. In sample A, 15Å of LTGaAs was inserted in the centre of a 150Å GaAs well. The growth was interrupted during the well growth to ramp down the temperature as described above. In sample B, just 3 monolayers of LTGaAs sandwiched by 4 monolayer thick confining barriers of AlAs grown at 600°C was inserted in the well. The structures are shown schematically in figure 1.

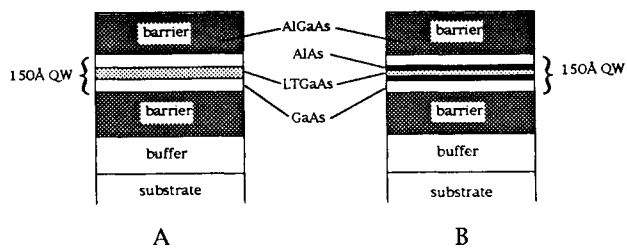

Figure 1

Schematic structure of samples A and B: The QW contains thin layers of LTGaAs. Sample B also has AlAs diffusion barriers. No PL was observed for either sample

Neither sample was specifically annealed after the LTGaAs layer was deposited, but growth of the upper barrier and completion of the structure means that both samples saw 600°C temperatures for 5 mins. No PL due to the well was observed in either sample, indicating that the density of non-radiative traps associated with these thin LTGaAs layers is sufficient to quench any detectable amount of radiative recombination. Since 1 at.% excess As translates into an enormously high defect density ($\sim 1 \times 10^{20}$ cm^{-3}) this may not be surprising. Yet, one might expect the defects to anneal out from such a thin LT layer as T_{sub} is raised. Obviously, this is not the case. Sample C contains no LTGaAs but was grown with a long growth interruption. It shows an intrinsic QW PL, confirming that unintentional impurity incorporation is not responsible for the PL quench.

The null result of samples A and B suggests that PL can be used to monitor the degree of As confinement by optically probing wells of unequal width surrounding a LTGaAs layer. This is the basis for the second series of growths and the results of samples D-H proved to be more interesting. The primary structure consists of three decoupled GaAs wells separated by 200Å thick barrier regions, as shown in figure 2. The first well to be grown is 150Å wide, followed by a 100Å well, and a 50Å well nearest to the surface. The upper and lower AlGaAs barriers are 500Å thick.

Sample H is a control sample. In this growth all three wells are grown at 600°C. There was no temperature ramping and no extended growth

interruptions. For samples D,E,F,G the 100Å well is grown at 230°C. In samples D and F, 30Å of AlAs is inserted in the 200Å thick barriers on either side of the LTGaAs layer in order to confine excess As. Samples D and E are annealed for 20 mins. at 600°C immediately following the central well in an As_4 flux of 5×10^{-6} torr, before proceeding with the remainder of the growth. Therefore significant redistribution of the LT-related defects is expected in these samples prior to the growth of the 50Å well. There is no anneal after the LTGaAs well in sample F or sample G. However, the remaining growth time for both samples is approximately 6 mins. at 600°C.

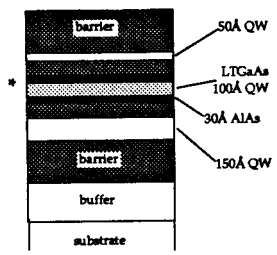

Figure 2

Growth structure for samples D-H: Three decoupled QW's, 50Å,100Å and 150Å wide. The middle (100Å) well is LTGaAs except in the control sample, H. Samples D and E are annealed for 20 mins. at 600°C following the 100Å well (*). The central barrier material in samples E and G does not include AlAs defect diffusion barriers.

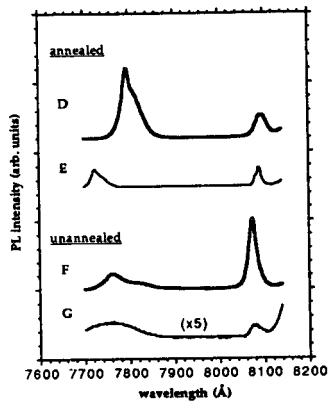

Figure 3

PL spectrum for samples D-G. D and E were annealed following the LTGaAs layer. D and F include AlAs diffusion barriers.Curves have been shifted vertically for clarity.The vertical scale has exaggerated by x5 for sample G.

The PL spectra corresponding to the four samples containing LTGaAs are shown in figure 3. Some PL due to the 150Å and 50Å wells are observed in all four samples. As expected, in no case do we detect PL due to the 100Å LTGaAs well itself. It is readily apparent that the presence of the LTGaAs layer has a significant effect on the quality of epilayers nearby.

The 50Å well double peak (due to monolayer fluctuations in the well-width) has broadened significantly in the unannealed samples which strongly suggests a degradation in the AlGaAs/GaAs interface quality. The optical efficiency of this well has also decreased compared to the annealed samples and the control sample, which suggests the introduction of non-radiative recombination centers in the well. These effects become increasingly large in sample G. In fact, the vertical scale has been exaggerated (x5) for sample G, and for this sample the peak is extremely broad (20 meV) and almost at the limit of detectability. In addition, there is a small (5-8 meV) shift in the peak position to higher energy for these two samples, with the magnitude of the shift being greater for sample G. (The seemingly large peak shift in sample E is an unfortunate artifact of barrier Al content. This sample was grown at a different

time in the MBE system cycle, whereas the other samples were grown consecutively). Previous studies on quantum wells grown on LTGaAs buffer layers have shown similar trends in peak shift to higher energy [6]. In that case, it was suggested that the presence of increasing strain due to higher concentration of excess As in the buffer layers was responsible for the observed energy shift. For the present growth structures, strain is an unlikely explanation. The LTGaAs layers are very thin and it has been shown that annealing at T_{sub}>580°C for 10 mins. is sufficient to remove the lattice mismatch to GaAs even for bulk layers of LTGaAs [4]. In this case, annealing at 600°C removes the source of the peak broadening mechanism. Both annealed samples, D and E, exhibit linewidths comparable to the control sample (10 meV). However, the effect of non-radiative traps remains significant in E, which contains no AlAs barriers. Nonetheless, this effect is reduced by the anneal.

In the case of the 150Å well, whose position in the growth means that it always sees unannealed LTGaAs, the effects are different. Again the optical efficiency of the well decreases compared to the control sample, with sample G having lowest efficiency. However, now sample F exhibits the highest intensity emission, comparable to the control. Interestingly, the linewidth is fairly uniform for all four samples (5 meV), indicating there is no induced interface disorder associated with backdiffusion from the LTGaAs layer. The decreased efficiency of the two annealed samples is probably due largely to the long anneal in an As_4 overpressure, rather than the LTGaAs.

We believe that there is a simple explanation for these results based on point defect considerations. When GaAs is grown at low temperatures, excess As is incorporated in the cystal implying a high concentration of As-rich related native defects, i.e. V_{Ga},As_{Int} and As_{Ga} type defects. Only the latter has been positively identified in LTGaAs [4], and then only for unannealed samples. As-related complexes are also likely to exist, to account for the remainder of the 1 at.% excess As. The thin LTGaAs layers in our growth structures are consequently highly localized sources of these defects in non-equilibrium concentrations..

As the lattice temperature is raised these native defects become more energetic and they will attempt to re-establish equilibrium concentrations. To do so, they must move through the crystal. Defect diffusion in III-V heterostructures has been extensively studied (readers are referred to review article by Deppe and Holonyak [8]). The observed broadening of the 50Å peak strongly suggests that the group III sublattice is involved in the forward diffusion defect migration mechanism. Therefore, we propose the following simple defect reaction as a possible first step in the redistribution mechanism for excess As in LTGaAs:

$$As_{Ga} \rightarrow V_{Ga} + As_{Int}$$

As the temperature increases many defect pairs of this type are created, with the reaction being driven by the highly non-equilibrium conditions. Typically the group III vacancy (V_{III}) defects have the highest diffusion rates of the six

possible native defects in III-V crystals. The V_{Ga} defects therefore can out-diffuse from the LT layer due to the concentration gradient much faster than the As_{int} defects. These vacancies will preferentially diffuse in the direction of the growth surface which is under an As_4 overpressure, since they can decrease the free energy of the crystal by self-annihilation at the surface. As they move forward through the crystal predominantly by hopping to adjacent group III sublattice sites they induce interface intermixing of group III atoms. The average Al content of the well increases (from zero) and that of the barrier material will decrease as the V_{III} moves across the GaAs/AlGaAs interface.This will inhomogeneously shift the 2D energy levels higher. This explains the broadening of the 50Å QW PL peak and its observed shift to higher energy in the unannealed samples. The ability to prevent such an effect may be of great importance in structures that are sensitive to interface-scattering or alloy-scattering effects. There is a relatively small effect due to vacancy outdiffusion observed in samples D and E because the anneal takes place immediately following the LTGaAs layer. The growth surface is therefore less than 40 lattice sites from the V_{Ga} defects which consequently find it easily. By the time the 50Å well is deposited, the native defect concentration of this type of defect is already at its equilibrium value.

AlAs layers were initially used as diffusion barriers because of the higher Al-As bond strength compared to Ga-As bonding. Since an Al atom must break its As bonds for the vacancy to propagate through AlAs, the V_{III} diffusion rate will be much lower in AlAs than in GaAs. Although sample F demonstrates that the 30Å AlAs barriers in our structures are not completely effective at preventing vacancy outdiffusion, they do offer a significant improvement over no barriers (sample G). Nevertheless, 30Å is a very thin layer, and thicker diffusion barriers can be expected to fully protect the integrity of epilayers grown on LTGaAs.

The 150Å well is not affected by V_{Ga}-induced intermixing since it is away from the preferential diffusion direction. The PL for this well does not display significant broadening effects. However, both wells display the effects of non-radiative recombination sites, which can be attributed to As_{int} defects and related complexes. As the temperature increases, their tendency is also to reduce the local non-equilibrium concentration. In this case the diffusion path involves hopping between neighboring interstitial sites or through some intermediate configuration involving mostly group V sublattice sites. Consequently we do not expect this type of defect motion to have a large effect on group III atomic positions. However, these defects do affect the optical efficiency of quantum wells when they are present by providing carrier trap centres. From our studies it is not clear which, if any, is the preferential diffusion direction for the As_{Int} type defects, although simple thermodynamics arguments suggest that backdiffusion would dominate for a sample in an As_4 overpressure. Indeed, the 150Å well data shows the PL quenching effect most clearly. In samples F and G we see that the insertion of AlAs barriers is definitely effective at inhibiting defect backdiffusion when we compare their optical efficiency.

Summary

We have studied the optical properties of thin layers of LTGaAs using PL measurements. Quantum wells containing even a few monolayers of material grown at 230°C were found to be optically dead which suggests the defects associated with LT growth are very effective at quenching radiative recombination. Outdiffusion and backdiffusion of these defects was investigated by their effect on nearby QW's. Group III atom intermixing effects is observed in the direction of the growth surface, which suggests that V_{Ga} defects due to the LTGaAs are involved in the defect migration mechanism. The insertion of AlAs barriers was found to significantly reduce the defect diffusion problem, being most effective against backdiffusion. Annealing the sample immediately following the LTGaAs improved outdiffusion effects by allowing defects to anneal out.

This work was supported by AFOSR. UKM was supported by a NSF PYI award.

References

[1]. F.W. Smith, A.R. Calawa, Chang-Lee Chen, M.J. Manfra, L.J. Mahoney IEEE Elec. Dev. Lett., vol.9, 77 (1988).

[2]. L.-W. Yin, Y. Hwang, J.H. Lee, R.M. Kolbas, R.J. Trew, U.K. Mishra, IEEE Elec. Dev. Lett., vol.11, 561 (1990).

[3]. J.M. Baranowski, Z. Lilienthal-Weber, W.-F. Yau, E.R. Weber, Phys. Rev. Lett., vol.66, 3079 (1991).

[4]. M. Kaminska, Z. Lilienthal-Weber, E.R. Weber, T. George, J.B. Kortwright, F.W. Smith, B-Y. Tsaur, A.R. Calawa, Appl. Phys. Lett., vol. 54, 1881 (1989).

[5]. A.C. Warren, J.M. Woodall, J.L. Freeouf, D. Grischkowsky, D.T. McInturff, M.R. Melloch, N. Otsuka, Appl. Phys. Lett., vol 57, 1331 (1990).

[6]. K.T. Shiralgi, R.A. Puechner, K.Y. Choi, R. Droopad, G.N. Maracas, J. Appl. Phys., vol.69, 7942 (1991).

[7]. J.P. Ibbetson, L.-W. Yin, U.K. Mishra, *to be published*

[8]. D.G. Deppe, N. Holonyak,Jr., J. Appl. Phys., vol.64, R93 (1988).

Inst. Phys. Conf. Ser. No 120: Chapter 2
Paper presented at Int. Symp. GaAs and Related Compounds, Seattle, 1991

Etching of GaAs and AlGaAs by H* radical produced with a tungsten filament

R. Kobayashi, K. Fujii, and F. Hasegawa

Institute of Materials Science, University of Tsukuba,
Tsukuba Science City, 305 Japan

Abstract: It was found that GaAs was etched with a smooth surface by radical or atomic hydrogen. The etching rate was as high as 15 um/h at the substrate temperature of 850°C and tungsten(W)-filament temperature of 2000°C. Several experimental results indicate that this high etching rate is due to evaporation of Ga as gallium hydride. Reaction between atomic hydrogen and AlGaAs was different from that for GaAs. Aluminum could not be removed so easily as Ga, and an aluminum oxide layer is left on the AlGaAs surface.

1.Introduction

The effects of atomic hydrogen on epitaxial growth or semiconductor surface is one of the recent topics. Noda et al. reported that a smoother surface was obtained when a platinum catalyst was placed beside the substrate in MOVPE of GaAs using triethylarsine (Noda et al. 1989). It is reported that selective growth can be achieved in MBE growth of GaAs if radical hydrogen is supplied on the growth surface (Yamamoto et al. 1989). Low-temperature cleaning of the substrate surface by atomic or radical hydrogen has also been reported (Sugata et al. 1988, Sugaya et al. 1991).

We have studied the reaction between $GaCl_3$ and arsine (AsH_3) or arsenic vapor from arsenic metal, and found that GaAs can be grown at much lower temperatures with AsH_3 than with arsenic vapor. This is because the hydrogen in the AsH_3 molecule is much more reactive than the hydrogen of H_2 (Kobayashi et al. 1990).

The first aim of this work was, therefore, to enhance the chloride VPE of AlGaAs at lower temperatures by generating atomic hydrogen without using the very toxic AsH_3. However, we found that the atomic hydrogen etches GaAs very quickly rather than enhancing the growth.

In this paper, we report the reaction of atomic hydrogen with GaAs and with AlGaAs.

2. Experimental

Figure 1 shows the schematic diagram of the experimental setup. The (100)-oriented GaAs substrate was put at three positions A, B and C on a carbon holder (distance between A, B and C is 2 cm each). The AlGaAs substrate grown by LPE was put at only the position B. The carbon holder was heated by an infrared lamp, and its temperature was monitored by a thermocouple inserted into the carbon holder.

The atomic hydrogen was produced by a heated tungsten (W) filament. This is the simplest method and has been successfully applied to the

growth of diamond films (Matsumoto et al. 1982). The diameter of the W-filament was 0.2 mm, and the length was 40 - 60 mm. The W-filament was positioned about 15-20 mm above the substrate. The temperature of the filament was estimated from the change in resistance, and was maintained at about 2000°C for most of the experiments.

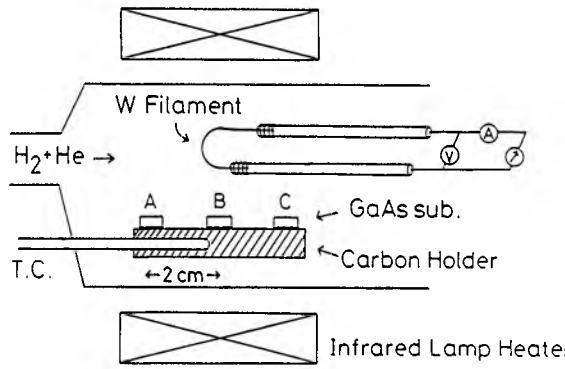

Fig.1 Schematic diagram of the experimental setup.

The experiment was performed in pure H_2 gas or (H_2 + He) gas mixture at atmospheric pressure. The gas flow rate was 180 sccm in a quartz reactor 45 mm in diameter.

Part of the substrate was covered by a small quartz chip. After etching, the chip was removed and the etched depth or the oxide thickness was measured by a surface profiler.

3. Experimental results and discussion

3.1 Etching of GaAs

A significant gas etching of GaAs substrates was observed when the W-filament was heated to 2000°C and the carbon holder temperature was kept at 850°C. The etching rate was about 15 um/h for the sample right under the W-filament, but the surface was rather smooth as shown in Fig.2(a). In order to confirm that this fast and smooth etching of the substrate is due

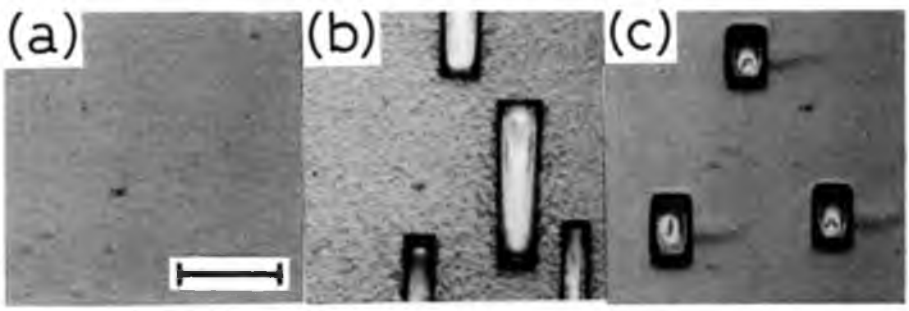

Fig.2 Surface morphology of GaAs substrates etched or annealed under various conditions ; (a) substrate temperature of 850°C and W-filament at 2000°C in pure H_2 for 60 min ; (b) annealed at 850°C for 60 min in pure He with W-filament of 2000°C; (c) annealed at 850°C for 20 min in pure H_2 without the heated W-filament. Marker represents 20 um.

to the radical or atomic hydrogen produced by the heated W-filament, the hydrogen partial pressure was changed by adding helium gas. The resultant dependence of the etching rate on the hydrogen partial pressure is shown in Fig.3. The etching rate decreases with a decrease of the hydrogen partial pressure, and it was about 3 um/h for pure helium (zero hydrogen partial pressure). The reason why etching was observed even in pure helium, is not properly understood at the moment; it might be due to the residual hydrogen or to mere evaporation of arsenic from the surface.

The etched surface becomes rough with a decrease of the hydrogen partial pressure, and many thermal pits with a gallium droplet inside appeared as shown in Fig.2(b). This rough surface is the same as is often seen for samples annealed in pure hydrogen without a heated W-filament. An example of such a surface is shown in Fig.2(c).

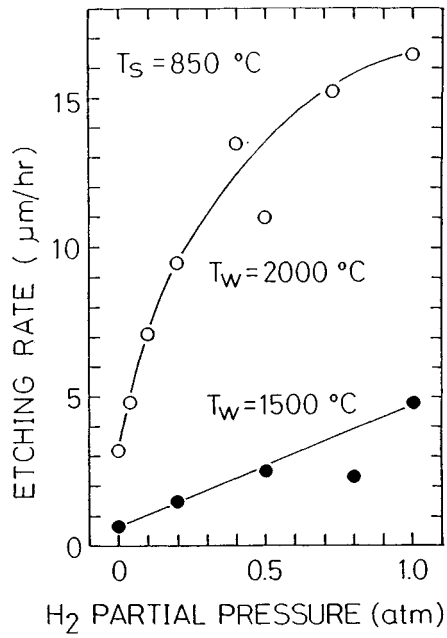

Fig.3 H_2 partial pressure dependence of the etching rate of GaAs by radical or atomic hydrogen.

The etching rate decreased very much with a decrease of the filament temperature from 2000°C to 1500°C. Still the same tendency of a decrease of the etching rate with a decrease of the hydrogen partial pressure was observed.

These facts indicate that the fast and smooth etching of GaAs is due to radical or atomic hydrogen produced by the heated W-filament: One might suspect an increase of the surface temperature due to radiation from the W-filament as the cause of the fast etching, but the temperature increase due to the radiation should be the same for different hydrogen partial pressure. Furthermore, when GaAs is heated in hydrogen or in vacuum, arsenic evaporates much faster than gallium, and gallium droplets are left on the surface as shown in Fig.2(c). There were no gallium droplets left on the surface when the sample was annealed in a hydrogen atmosphere with a heated W-filament. It was also confirmed that the gallium droplets left on the GaAs surface could be removed by annealing with the heated W-filament (Kobayashi et al. 1991). This fact suggests that the gallium is evaporated as a hydride by the radical or atomic hydrogen produced by the W-filament. Existence of gallium hydride and aluminum hydride is reported in rather old papers (Wiberg et al. 1942, Finholt et al. 1947). Therefore, it is not unreasonable to assume that gallium is removed as gallium hydride by radical or atomic hydrogen.

3.2 Transport of GaAs by atomic hydrogen

The sample right under the W-filament was always etched, but when the substrate temperature was not very high, both etching and deposition

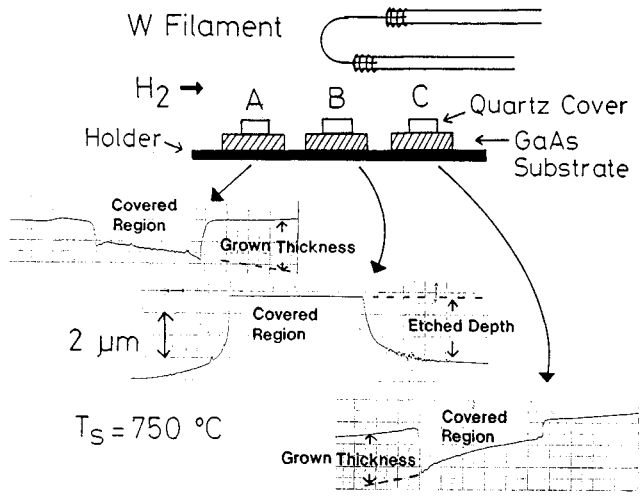

Fig.4 Surface profile of each GaAs substrate measured by a surface profiler. The carbon holder was about 750°C and etching or deposition time was 60 min.

of GaAs was observed. Figure 4 shows an example of such case. The top half of the figure shows the configuration of the experiment and the bottom three curves show the surface profiles of the GaAs samples placed at positions A, B and C of the carbon holder separating by about 2 cm. Center of each profile is the portion covered by a quartz chip. The carbon holder was 750°C, and the W-filament was 2000°C.

The sample placed at position B (right under the W-filament) was etched, but deposition rather than etching was observed on the samples placed at positions A and C. Since there is no GaAs source other than the sample placed at position B, this fact indicates the transport of GaAs from the sample at the center(B) to the samples at the both sides(A and C). This phenomenon would be explained as follows: Density of the atomic hydrogen must be higher at the center (position B) than at both sides (positions A and C), therefore, arsenic and the gallium evaporated from the center sample as gallium hydride diffuse to both sides. Since gallium hydride is unstable, the gallium deposited in arsenic vapor and GaAs was grown on the substrates placed at positions A and C.

Since the vapor pressure of gallium is very low even at 900°C, this fact also indicates that the gallium is evaporated as a hydride by the atomic hydrogen, otherwise a high rate transport of GaAs shown in Fig.4 under a pure hydrogen atmosphere can not be understood.

3.3 Etching of AlGaAs

In order to see reaction between atomic hydrogen and AlGaAs, the same experiments were performed using LPE grown AlGaAs with Al content of 30%. Figure 5 shows the experimental results.

The results for AlGaAs was quite different from those for GaAs.

First of all, AlGaAs is never thermally etched. Even when it is annealed at 900°C in pure hydrogen gas without a heated W-filament, the surface is smooth without any thermal pit. Of course no gallium droplet is left. Instead of that, the surface is slightly oxidized.

When the atomic hydrogen is supplied, the AlGaAs layer is etched as shown at the top of the figure, but a thick aluminum oxide layer is left on the surface.

The solid circle of the figure shows thickness of the oxide layer left after etching by atomic hydrogen and the open circle shows the total etched depth after removing the oxide layer against the etching time. Both the total etched depth and the oxide layer thickness increase almost linearly with an increase of the etching time. However, thickness of the oxide layer is almost the same as the etched depth, suggesting that only gallium and arsenic are etched by the atomic hydrogen, and aluminum is left behind.

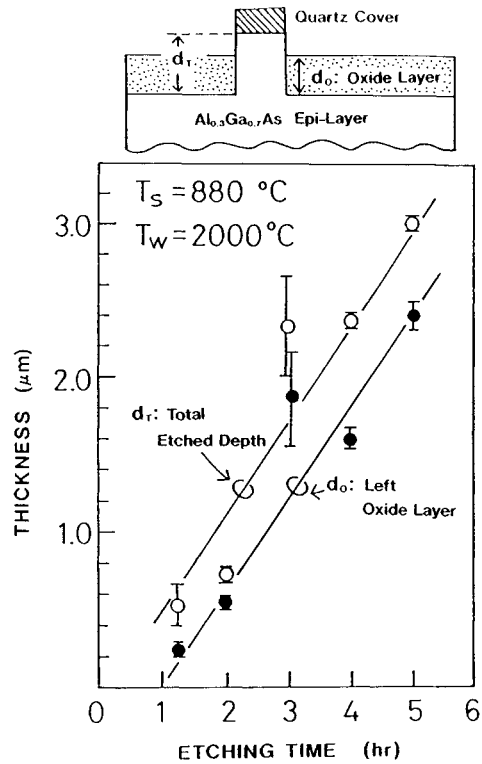

Fig.5 Dependence of the oxide layer thickness after etching and the total depth after removal of the oxide layer on the etching time for LPE grown AlGaAs.

Since the reactor used here is not an ultra high vacuum type, there must be slight leakage. Therefore, when gallium is removed by the atomic hydrogen, aluminum left on the surface must have been easily oxidized and a thick oxide layer was formed. Thickness of the oxide layer increases linearly with an increase of the etching time, but it does not go through the zero point. This fact might indicate that aluminum is also slightly removed as aluminum hydride by atomic hydrogen, at least at the beginning of the etching. Further experiments in an ultra high vacuum type system is necessary to conclude whether atomic hydrogen really reacts with aluminum and evaporates as a hydride or not.

4. Conclusion

It was found that GaAs was etched with a smooth surface by atomic hydrogen. The etching rate was as high as 15 um/h at substrate temperature of 850°C and W-filament temperature of 2000°C. When the temperature of the carbon holder was relatively low, transport of GaAs from the sample near the W-filament to substrates distant from the filament was observed. These results suggest that gallium on the GaAs surface is removed as a hydride by radical or atomic hydrogen generated by the W-filament.

As to reactions between atomic hydrogen and AlGaAs, aluminum could